Effect of combined dry-wet irrigation and microbial dynamics on soil nutrient bioavailability

Arnab Majumdar[1]* (arnabmajumdar891@gmail.com), Munish Kumar Upadhyay[2] (munish007up@gmail.com), Pradeep Kumar Dubey[3] (pradeep.dubey4@bhu.ac.in), Biswajit Giri[1] (giri.biswajit605@gmail.com), Ashish Kumar Srivastava[4] (ashishbarc@gmail.com), Sudhakar Srivastava[5] (Sudhakar.srivastava@gmail.com)

[1]Department of Earth Sciences, Indian Institute of Science Education and Research (IISER) Kolkata, Mohanpur, West Bengal 741246, India

[2]Environmental Geochemistry Laboratory, Department of Civil Engineering, Indian Institute of Technology Kanpur, Uttar Pradesh 208016, India

[3]Institute of Environment & Sustainable Development, Banaras Hindu University, Varanasi 221005, India

[4]Nuclear Agriculture and Biotechnology Division, Bhabha Atomic Research Centre, Mumbai 400085, India

[5]Plant Stress Biology Laboratory, Institute of Environment & Sustainable Development, Banaras Hindu University, Varanasi 221005, India

*Correspondence- Dr. Arnab Majumdar (arnabmajumdar891@gmail.com)

The manuscript has submitted to 'Agronomy Journal', a member journal of the American Society of Agronomy, and been revised based on one round of peer review, but has yet to be formally accepted for publication. The authors are currently preparing additional revisions, and thus subsequent versions of the manuscript will have different content.

Abstract

Alternate wetting-drying (AWD) cultivation with implication on soil microbiome, nutritional dynamics and rice yield during pre-monsoon (boro) and monsoon (aman) season are not well studied. In the present 4-year field study the impact of AWD (in pre-monsoon season) is compared with conventional mode of irrigation (i.e. flooded field in monsoon season). The release of soil nutrients into the soil-aqueous system, influencing microbial populations and modulating the redox status were explored. Results indicated an increase in total content as well as bioavailability of selected nutritional elements (N, P, K, Fe, Ca, Mg, Cu and Zn) by 16-54% in the pre-monsoon cultivation relative to monsoon cultivation. Three plant growth phases (developing, milking and harvest) were considered to check the nutrient modulations in soil and plant tissues along the continuum plant growth and elemental uptake. Krona charts, relative abundance, rarefaction curve and multivariate analysis of metagenomics data showed that the pre-monsoon soil was more enriched and maintained a balance between soil pH and microbial biomass than the monsoon soil. Microbial community diversity associated with plant growth phases also found to be different depending on the seasonal alterations. *Bacillus* sp., *Acidothiobacillus* sp., *Pseudomonas* sp., *Rhizobium* sp., *Burkholderia* sp. were predominant in pre-monsoon soil releasing pulses of N, P, K, Ca and Mg whereas Verrucomicrobia was found to be dominant in monsoon soil where Fe was released. This study is a first of its kind that showed the combined effect of season and soil microbes on macro-micro nutritional availability in soil and enhanced plant quality.

Keywords: Soil quality; Metagenomics; Nutrient availability; Pre-monsoon irrigation; Resource conservation; Soil microbiome

Introduction

Upto 43% of global irrigation water (accounting nearly 27% freshwater available on the planet) is directly consumed for rice production. The estimated average consumption of 2500 litres of water for a kilogram of rice produced is huge water footprint for global rice production (Surendran et al., 2021). However, since rice is a staple food crop for nearly half of world population and source of livelihood for hundreds of millions of farmers across globe, therefore, devising sustainable ways of rice irrigation under changing climate scenario is highly imperative (Majumdar and Bose, 2017; Dubey et al., 2020). These variable strategies adopted for rice cultivation depends on site specific edaphic factors, soil physico-chemical properties and prevailing environmental conditions(Majumdar et al., 2020a; b). The informal pump irrigation is largely a contingent water source for a boro season rice cultivation in regions like West Bengal in India and in other South Asian countries like Bangladesh etc. Overreliance on groundwater for irrigating paddy field in boro season (i.e. during pre-monsoon period) primarily causes groundwater depletion (Dangar et al., 2021; Tulip et al., 2022), aquifer havoc further adding to the existing regional Arsenic toxicity challenges (Nickson et al., 2000; Johannesson and Neumann, 2013; Kumarathilaka et al., 2018), as well as unsustainable usage of non-renewable forms of energy (as diesel/fuel) and power (electricity) (Mukherji, 2007). Hence, unravelling water resource conserving agronomic practices for rice cultivation majorly during boro season holds paramount importance owing to its environmental merits in response to changing climate, as well as safeguarding the energy-irrigation nexus (Dubey et al., 2020; Surendran et al., 2021). In this backdrop, alternate wetting and drying mode of irrigation, raised beds, system of rice intensification (SRI) techniques, or saturated soil culture (SSC), ground cover system, or aerobic rice cultivation etc. has already gained scientific momentum and is cited in several recent field-based studies done in West Bengal, Bangladesh and adjacent regions (Baldwin and Mitchell, 2000; Venterink et al., 2002; Blackwell et al., 2010; Dodd et al., 2015; Surendran et al., 2021). Moreover, the agrarian population in the region are also partly convinced in adopting irrigation method such as alternate wetting and drying of paddy soil, especially during boro season as an adaptive rice cultivation practice (Pearson et al., 2018; Majumdar et al., 2021; Upadhyay et al., 2022). So far, the site-specific motives attached to adoption of AWD irrigation mode are the water resource crunch faced by large segment of subsistence rice farmers during the peak season requirements and the erratic weather pattern witnessed over preceding years due to changing climate (Pearson et al., 2018; Dubey et al., 2020).

However, in present study we have explored the implications of alternate wetting and drying of paddy soil during boro season on variations in soil microbiome and their nutritional dynamics.

The drying of paddy field soil followed by subsequent re-watering enhances rice productivity through with flushes of nutrient release to the soil influencing soil microbial populations (Baldwin and Mitchell, 2000; Dodd et al., 2015). The rotation of drying and re-watering process in pre-monsoonal dry season can influence the soil organic matter (SOM) mineralization and microbial turnover; known as the 'Birch Effect' (Birch, 1958). This effect has been observed for available C, N and P released in soils (Mikha et al., 2005; Blackwell et al., 2010; Mooshammer et al., 2017). The re-watering practice influences the pre-monsoonal soil nutritional flux while affecting the microbial load (Wu and Brookes, 2005; Xiang et al., 2008). However, the direct effect of such seasonal variation and physico-chemical changes on microbial populations for other essential nutrients like Fe, Ca, Mg, Cu and Zn had not been studied. This cycle of drying and rewatering soil during pre-monsoonal wintry-summer season induces the release of intra-cellular osmolytes like amino acids, ammonium compounds, glycerol and other organic solutes to the extracellular environment (Wang et al., 2017; Majumdar, 2021). In monsoon soil, a slower microbial decomposition of organic matter was reportedly due to the lower requirement of N in anaerobic metabolism (Nishio et al., 1994). During the re-watering process of wintry dry soil, water gets entrapped within the soil aggregates leading to the better availability of soil organic matter (SOM) for microbial decomposition which allows microbes to break down recalcitrant complexes and release nutrient flushes to the soil (Miller et al., 2005; Wu and Brookes, 2005).

There is a dearth of study showcasing the effects of employing water resource conserving practices during one rice season (i.e. pre-monsoon boro rice season under the boro-aman rice cropping pattern) on the nutrient availability and soil microbial community together. Therefore, an exclusive long term four-year field study (starting from February-May 2016 and extended till July-October 2019) were conducted in West Bengal, India unrevealing the positive implications of alternate wetting drying irrigation method (employed during boro season) on soil microbial dynamics (applying metagenomic applications) and nutrients bioavailability improving the crop and system yield. Overall, the merits of aforementioned water resource conserving agronomic practice in comparison with conventional monsoonal waterlog system is comparatively evaluated. Moreover, saving critical natural resources in agriculture such as water and soil have direct and indirect

interlinkages with several United Nations Sustainable Development Goals (UN-SDGs) and their target set for year 2030 (Dubey et al., 2021a; b, 2022; Huang et al., 2021).

Materials and methods

Study area and experimental field set up, sample processing and analysis

The study area, Katwa block (latitude 23°43'25.4"N, longitude 88°01'30.4"E) of Bardhhaman district, West Bengal had been selected based on our earlier assessment and soil As tracing (Majumdar, A., 2016-2019, unpublished data; (Laha et al., 2013). For a long-term study of the effect of pre-monsoon cultivation, wintery-summer (boro) and rainy (aman) season was selected for four consecutive years from 2016 to 2019. Three fields, 1800 square feet each, were selected for cultivation and soil-plant sampling based on randomized block design to avoid any partiality. The fields was selected based on the pattern of cultivation practiced locally for over two decades using pond water only. Water depth was maintained at 30cm from the surface soil in the monsoon field. In the pre-monsoon cycle, pond water was applied at the beginning and retained for 2 days with subsequent release of the water from the field, drying for the next 10 days, making the soil moisture reduced to 60% of saturated values, and the field was monsoon again. This drying-wetting cycle was continued till the rice grain milking stage followed by a semi-dried phase (50% saturation) till harvesting. Soil and rice plant samples were collected at three phases- pre-mature or developing, milking or grain filling stage and mature or harvesting stage.

The collection, processing of soils, sample preparation and analysis were conducted using wavelength dispersive X-ray fluorescence spectroscopy (WD-XRF, Tiger S8 Bruker) by following the method described in (Majumdar et al., 2018, 2021). Soil samples were analyzed for the physico-chemical properties like pH, redox potential (ORP) using Oakton Waterproof PCS Testr35 and ORP Testr 10 and total organic matter by following the Walkley and Black method(Walkley and Black, 1934). On-spot field observation of soil pH and ORP was also done to check for any changes in the collected samples. Four standard reference materials (SRMs) (SBC-1, GSP-2, MESS3 and NIST2711a) were used for optimized calibration with an 82-91% recovery rate. Instrumentation specifications have been mentioned in **Supplementary Table 3**. Total N content was measured by following the Kjeldahl method. Soil samples were also tested for the bioavailable fractions of the selected elements by using an inductively coupled plasma mass

spectrometer (ICP-MS, Parkin-Elmer)(Ray Sarkar et al., 2017; Shrivastava et al., 2020). Instrument specifications are given in **Supplementary Table 2.** The detailed process and chemicals used are mentioned in **Supplementary Table 1**.

Rice seeds (Pusa Basmati 1121) were kept moist for one week to germinate and then grown in the nursery until the seedlings (around 20 days after germination) were transferred to the respective fields. Plant samples were collected 18-20 days after the transfer to the field and were marked as 'developing'. After 40-45 days of first sampling, plants were collected during the milking phase and after the seeds were ripened, final sampling was done at harvesting time. A destructive method of di-acid digestion was followed after complete drying of plants at 60ºC for 4-5 days, for the total elemental content measurement in plant samples using ICP-MS (Majumdar et al., 2019, 2022).

DNA extraction from soil and metagenomics analysis

A small amount of soil was used for the DNA isolation using QiagenDNeasy Powersoil Kit (Cat#12888). The study considered soils from inflorescence and harvesting phase, due to differed water saturation and nutrient contents available. Region-specific targeting proprietary primers at Genotypic Technology Pvt. Ltd., Bangalore, India, were used for all the metagenomics analysis and V3-V4 metagenome library preparation. All the detailed processes have been mentioned in the **Supplementary file**. V3-V4 primer sequences from the Illumina paired-end raw reads were selected from the high-quality bases. RDP6 classifier was used to assign taxonomies with clustered at ≥97% sequence similarities while comparing to the Greengene database which created a biome file. This biome file was further used for advanced analysis and visualization. Alpha and beta diversity for microbial species richness was calculated for each sample. Krona charts were made that are interactive html files consisting of the phylogenetic information at each taxonomic level. Venn diagram, multivariate analysis, rarefaction plot, were made to identify the difference in microbial diversity in different soil samples. Cytoscape (var. 3.8.2) was used for the microbial network distribution based on the elemental content in soil, assigned as 'edges' and read counts of classes were assigned to be 'target nodes' for generating this network.

Statistical analysis of soil-microbe data

All the experimental data of soil analysis for total and bioavailable elemental concentrations were justified by analysis of variance (ANOVA) at $P<0.05$ significance level. Duncan multiple range

test (DMRT) was also used for the level of significance and inter-class variance identification. Principal component analysis (PCA) and principal coordinate analysis (PCoA) were used to justify the distribution pattern assessment in soil samples and inter-elemental relation along with the microbial species distribution within the soil samples from altered seasons. Graphpad Prism 6, SigmaPlot (ver. 12) and PAST (ver. 3.2.1) were used for the graphical and statistical analysis.

Results

Soil assessment for nutritional profiling and plant accumulation under altered irrigation

Soil samples from two altered seasons (monsoon and pre-monsoon) at three sampling time points (developing, milking and harvest) were assessed for the total elemental concentration and obtained results are presented in **Fig. 1** as radar plots. This radar plot is a constrictive layered formation with major and minor grids indicating the major concentration bands and sub-divisional concentration bands within sampling phases which eases multi-parameter data comparison. The blue line in the figure corresponds to the connecting pattern in changes of concentration in different fields. In all the years, 2016-2019, soil samples from the harvest phase always showed the highest amounts of nutrients irrespective of cultivation processes. However, differences were evident when monsoon soil was compared to the pre-monsoon soil where the deposition of elemental content was highest (**Fig. 1**). Sub-divisions of the radar plot in each year showed a fluctuation in the concentration pattern between the developing and harvest phase. From 2016 to 2019, the increment in concentrations of total N, Ca, K, Mg, Fe, P, Cu and Zn were 38.6%, 38.0%, 4.4%, 37.3%, 12.4%, 24.3%, 54.7% and 36.9% respectively while comparing element contents in control soil to pre-monsoon soil. Whereas the percent increments were 45.98%, 56.4%, 19.7, 38.9%, 16.1%, 30.4%, 64.3% and 54.4 % of N, Ca, K, Mg, Fe, P, Cu and Zn, respectively, in pre-monsoon soil in comparison to the monsoon soil (**Fig. 1a to 1d**). The total content increased by the end of 2019 sampling. **Fig. 2** shows the total nutrient enrichment in whole rice plants by summing the root and shoot content from three different fields. Rice can alter the uptake of nutrients from the soil dependent on the levels of supply and the demands of growth (Hasanuzzaman et al., 2018; Afsal et al., 2020; Gupta et al., 2022). **Fig. 2a-h** shows a similar trend in elemental accumulation in plants under altered seasonal cultivations. Groundwater application enhances the soil nutrient concentrations but flooding flushed out nutrients from the field resulting in a low elemental profile in rice grown under these conditions. An increase in elemental concentrations was observed in pre-

monsoon plants from 2016 to the end of 2019 at the harvesting phase. Except for Na (-28.95% in monsoon to pre-monsoon), all other nutrients showed a positive increment. Comparing monsoon soil to pre-monsoon soil the percent increases were 55.6%, 58.6%, 32.2%, 51.2%, 52.8%, 31.3%, and 38.6% for Ca, K, Mg, Fe, P, Cu and Zn respectively at the harvesting phase. Plant's elemental concentration at the pre-mature and milking phases had a similar accumulation trend as at the harvesting stage.

Soil physico-chemical influence on nutrient bioavailability and yield enhancement

In paddy fields, the soil pH and redox potential (ORP) show an opposite correlation(Kabata-Pendias, 2000) that influences the soil elemental concentration by modulating the inter-relationships of soil elements. **Fig. 3** shows the correlation matrix plot for soil physico-chemical parameters and nutrients. **Fig. 3a, b** and **c** correspond to the analysed soils from developing, milking and harvest, justified based on the three algorithmic representations- shape (degree of an oval to ellipsoid), color (dark red to violet) and directions (upward or downward) to show the positive to negative correlation with statistically valid range marked as grey colored boxes. Higher content of organic matter was observed in the developing phase, this also showed a strong positive correlation with soil pH changes but no such relationship was observed with ORP. In the rice field, the availability of P depends on both natural soil amounts and applied fertilizer levels and that makes a strong association with soil pH and OM in the developing phase. Although both pH and ORP revealed a negative relation with other nutrients, SOM influenced positively some of the elements like P, Cu and Zn. Iron complexes are stable under high OM(Kabata-Pendias, 2000) and total Fe showed a negative association along with Mg and K (see Fig. 3). In milking and harvest phase soils, SOM was found to be lower than in the developing phase, but pH and ORP was highly variable and a showed negative relationship. Water logging in the monsoon soils has lowered pH and ORP values when compare with the pre-monsoon field. Redox potential changed positively the available content of Mg, Fe, P and Cu whereas the rest of the elements were found negatively correlated. Among inter-elemental dependences, Ca, Mg, Cu and Zn showed positive relationships with all other elements. Soil nutritional status confers significant plant growth and final grain yield after the harvesting phase and as shown in the **Fig. 3d**, total yield (calculated per hectare) was found to be increasing yearly, although at marginal difference, but greater than the monsoonal

flooded fields. The yield percent increment was 6.46% in pre-monsoon boro cultivation and 5.2% in monsoonal aman cultivation.

Bioavailable elemental distribution in fields is influenced by pH and microbial biomass

Soil pH and microbial activity are very closely related as both depend on the soil moisture content, SOM and under altered drying-wetting irrigation in pre-monsoon cultivation, higher content of microbial biomass carbon (MBC) and alkaline soil pH was observed(Bickel and Or, 2020; Majumdar et al., 2021). In this study, successive observations of soil pH and MBC in all four years were assessed (**Fig. 4**). The contour map is a complex yet important plot to show the elemental distribution in a field experiment with color coding from low to high. Each of the plots in **Fig. 4** consisted of combined data from four years of harvesting time points from the three different phases. The total microbial load was found to be the highest at this phase as shown in **Supplementary Fig. 1.** The bioavailable concentration of each element was selected as the 'z-axis' or the distribution axis. A single plot contained soil pH, MBC data and bioavailable nutrient contents for the three fields. In these plots the distribution of any element can be depicted from the data range of MBC and pH from the different fields. For example, the distribution of N in the figure can be seen to be higher near the contour region of MBC 3.3 to 3.8 mg, corresponding to the pre-monsoon field soil, spanning to a wide range of soil pH. This indicated the higher N availability at higher microbial biomass enriched soil of pre-monsoon fields. A comparatively lower MBC corresponds with less available N in the soil within the same pH range in control or monsoon fields. Similar results were found in the case of Ca, Mg and P distribution in three field soils where higher MBC in pre-monsoon soil resulted in higher available elemental concentration. The K availability was different to this trend possibly due to the greater requirement of K for microbial growth and metabolic activity(Parmar and Sindhu, 2013). Hence, the lower MBC content in soil resulted in higher available K in monsoon soils relative to the pre-monsoon soil. With increasing pH, the availability of K also increased in pre-monsoon fields under low MBC content. For Fe, the distribution was more or less similar to the K due to the redox changes and utility of Fe by microbe's growth(Liesack et al., 2000; Jia et al., 2020). MBC within a range of 2.5 to 3 mg in monsoon soil had the highest range of available Fe compare to the control or pre-monsoon soils. The circulation of Cu and Zn was similar and only a higher range of MBC showed

the highest availability of these two micronutrients in pre-monsoon soil, irrespective of the soil pH.

Principal components and statistical analysis of field soils

PCA plots with bi-plot distribution of selected elements within soils at three different sampling phases have been shown in **Fig. 5**. In 2016, the pre-monsoon soil at the final phase of soil sampling revealed the most variance in elemental content specifically K and Fe, whereas P, Ca and Mg were more influenced during the beginning and middle of the cultivation in pre-monsoon field soil (+PC1, +PC2). Compared to the pre-monsoon soils, monsoon soils were found to be less statistically varied (-PC1, +PC2). The PCA analysis of 2017 data was different from the previous plot in terms of elemental bi-plot distribution where most of the elements except P, showed high variability at pre-monsoon harvest soils. Other monsoon soil data fall within either the (-PC1, +PC2) or (-PC1, -PC2) quadrant. The propagation of selected elements in all the field soils in 2018 followed the same trend as in 2017. In the next year, the total elemental distribution bi-plot was found to be the same but the PCA of field soils were variable. In 2019, the self-variance in the data of pre-monsoon soil was observed as distributed in (+PC1, -PC2) to (+PC1, +PC2) quadrant. Among the fields sampled, pre-monsoon field mainly constructed the PC1 and the discreet data from control and monsoon makes PC2, depending on the concentration gradient and consecutive distribution in those fields. Apart from the PCA, all the data from different fields and sampling phases were statistically tested using one-way analysis of variance (ANOVA) at $p<0.05$. All the data were found significantly variable and independent to each other.

Metagenomics analysis of soil and nutrition modulation

Changed microbial diversity abundance under altered water regime

The total phylum diversity in the soil after Illumina next generation sequencing metagenomics analysis has been shown in **Supplementary Fig. 1**. The pie chart showed the predominance of different phyla present in the three analyzed soils. In developing soil, the Proteobacteria accounted for 33.7% followed by Acidobacteria 20%, Planctomycetes 9.8%, Chloroflexi 8.3%, Nitrospirae 6.7%, Actinobacteria 5.4%, Bacteroidetes 5.2%, Gemmatimonadetes 3.4%, Verrucomicrobia 2.9% and Firmicutes 1.7%. Apart from these dominating phyla, some other key phyla like cyanobacteria were identified, although in lesser abundance (see **Supplementary Fig. 1a** with

respective read counts). Soil samples from milking and harvest soils had more varied phyla compared to the developing soil, as presented in **Supplementary Fig. 1b** and **1c** respectively. Proteobacteria were appraised as 37.0% and 31.0% in monsoon and pre-monsoon soils. Chloroflexi 24.4% was the second most dominating phylum in pre-monsoon soil followed by Acidobacteria 15.47%, Nitrospirae 7.44%, Actinobacteria 4.72%, Planctomycetes 4.06%, Bacteroidetes 3.32% and Verruocomicrobia 1.16%. In the monsoon soil, the community differed by Chloroflexi 16.8%, Acidobacteria 13.04%, Nitrospirae 7.33%, Bacteoidetes 6.36%, Actinobacteria 5.11%, Planctomycetes 4.28%, Verrucomicrobia 2.19%, Cyanobacteria 1.63% and Gemmatimonadetes 1.15%. **Supplementary Fig. 2** shows the microbial class distribution in three soil samples with respective dominance and availability in the soil as counted in the metagenomics assessment. From the color code, the maximum and minimum dominance can be seen and from the size of the circle, the degree of availability can be understood. Alpha- and Betaproteobacteia were dominant in harvest soil whereas Gamma- and Deltaproteobacteria were dominant respectively in developing and milking soil phases.

Phylogenic interaction and nutrition modulation in soil

Microbial inter-relation in the soil environment represented by a krona chart for all the three soils (**Fig. 6**), that helps in the visualization and exploration of relative abundances in all the phylogenic levels of microbial classifications, generated in HTML format. This krona chart creates a radial space-filled multi-layered colored plot with interactive zooming to each of the phylogenic levels analyzed for the overall microbial community(Ondov et al., 2011). **Fig. 6** represents a general graphical form where bacterial and archaeal communities are in different shades of color. Also, from these three kronas, it was observed that the presence of archaea was higher in the milking and harvesting phase soils, mostly related to anaerobic methanogenic species, compared to the developing phase soils. Influence of pre-monsoon (**a, b, c**) was also clearly found to be greater than the monsoonal soils (**a1, b1, c1**). Microbial count of some specific groups present in monsoon soil was higher than the other soil samples. But dominating this quantitative data, the nutritional release in the pre-monsoon soil was higher due to the combined effects of the irrigation process and heterogeneous microbial metabolic activities as it depicts the differences in alpha diversity by comparing the library sizes for each of the samples, whereas beta diversity elucidates the species richness within an ecological community. **Supplementary Table 4** shows the analyzed alpha and

beta diversity indices for all three soil samples. The inter-ecological community comparison is generally made by calculating the beta diversity and from the observed results, both alpha and beta diversity showed that the pre-monsoon soil had higher species richness due to the changes in irrigation practices and nutrient availability. Statistical approach justifies the metagenomics results for the monsoon soil having variable soil conditions leading towards an unstable microbial community compared to pre-monsoon soil. The species-specific dependency of each microbial species had been analyzed by principal component (PCA) and principal coordinate analysis (PCoA) as in **Supplementary Fig. 3**. PCA analysed in a bi-plot model and among the three-phase soil microbiome, developing microbiota was placed in the first quadrant (+PC1, +PC2) whereas harvest and milking biome placed into the fourth quadrant (+PC1, -PC2). PCoA suggests the dissimilarities between samples analyzing the ordination space with a linear mapping of Euclidean data and the observed variance within the original data (Ramette, 2007). The metagenomics data presented here showed that most of the species' occurrence was centric to the plot and some of the discrete points were dispersed and found to be unidentified species of microbes. **Fig. 7** shows an interactive microbial network analysis depending on the soil nutrient content and dispersion in the field. During data loading and the network formation, microbial phylum and classes were accounted with their specific encountered numeric values in the metagenomic sequence analysis along with soil elemental concentrations. Microbial phyla were selected as source nodes while microbial classes were selected as target nodes. Numeric values for each set of the field microbial data were selected as target edge attribute followed by elemental concentration data as target node attribute. The resulted network shows microbial classes interacting with each other while modulating the nutrients content in soil.

Discussion

Plants were cultivated using stored pond water, that itself is not elementally enriched in nutrients(Shrivastava et al., 2014) and application of such surface water did not increase the elemental content any further except the natural redox de-coupling of elements from soil complexes. The water application to dry soil releases nutrients to the soil-aqueous phase (Venterink et al., 2002) that in turn can induce the microbial metabolic activity, exchange of electrolytes in soil, changing the redox status of different elements and hence, the bioavailability for crops changes (Miller et al., 2005; Wu and Brookes, 2005). Some reports suggest that the

mineralization of N increases during the drying phase after the water drainage with increasing soil aeration and subsequent denitrification occurring in semi-dry soil(Fageria et al., 2010; Lu et al., 2020). The combination of these two processes leads to the increased bioavailability of soil N to the plant system. The flushing out of surface soil elemental complexes increased the chance of electrolyte release into the stagnant water(Majumdar et al., 2019; Upadhyay et al., 2021). A prevailing soil aqueous phase with lower ORP values and reductive environment can alter the Fe-redox state(Majumdar and Bose, 2018) and this conversion will influence the available content of Fe along with other nutritional elements in a monsoon field. In soil, the availability of P and K depends on the drained water that controls the physical adsorption and chemical equilibria of these elements on either soil particles or other elemental complexes(Parmar and Sindhu, 2013; Song et al., 2021). Hence, the soluble content of K is more available to the plant systems under waterlogged soil compared to the semi-arid soil. Although, soluble P (inorganic forms) are easily available to the plant system and due to the consecutive re-watering of dry fields, this extractable P content becomes around 40% higher than in longer-term monsoon fields(Bünemann et al., 2013). SOM plays an important role in the association of Cu and Zn to other elemental complexes and controls the bioavailability(Fageria et al., 2010). Hence, the bioavailability of Cu and Zn in control and pre-monsoon field soil was higher than the monsoon soil (see Fig. 3). The distribution of Cu and Zn, hence, was higher in the region of high MBC (Fig. 4) which corresponds to the pre-monsoon field throughout the pH ranges. In soil, nutrient dissolution from complexes and bioavailable nutrient pools are crucial factors that influence soil microbial biomass and in turn, their heterogenic metabolic activities under neutral pH and temperature(Leita et al., 1999; Wang et al., 2016; Zhou et al., 2020). More availability of these macro-micronutrients in soil under pre-monsoonal wetting-drying conditions helps crop growth and yield better than the flooded condition at monsoonal season (Fig. 3). Harvest index by calculating the plant leaf area, tiller numbers, root to shoot lengths and panicle numbers were found to be greater under the AWD cultivation (data not shown). Microbial biomass stoichiometry and community composition can variably perform soil nutrient mineralization and immobilization to influence soil fertility(Heuck et al., 2015; Delgado-Baquerizo et al., 2016). Under pre-monsoonal drying-wetting cycles in fields, the intermittent water application at certain times enhances the available soil C-N-P pool and help soil microbes grow better than under continuously monsoon soil.

From the metagenomics data, it can be seen that the encountered reads of occurrence of a single species or genus were higher in monsoon soil but the overall species diversity was greater in pre-monsoon soil. The species richness has confirmed that the harvesting phase had a greater community diversity which can modulate the nutrient pool to a greater extent as shown in the Fig. 4. Chloroflexi is such a metabolically heterogeneous group of phyla that consists of both anoxygenic-photoautotrophy as well as oxygenic chemoheterotrophy(Gupta, 2013). The high percentage of Chloroflexi in the pre-monsoon soils indicate the semi-aerobic cultivation with possibly abundant nutritional pulses enhanced by the Chloroflexi growth. In pre-monsoon drying-wetting, a subtle change of pH and redox potential during the water content alteration resulted in the release of available N, P, K, Ca and Mg that could have triggered the predominance of another metabolically diverse microbial phylum Acidobacterium. Like Proteobacteria, this phylum can also thrive under the differential supply of macro-micronutrients in soils, stimulating the conversion of soil nitrite and nitrate, various types of organic matter and carbohydrate utilization(Kielak et al., 2016). These two phyla are also present in the monsoon soils although at the lower abundance. The higher predominance of Cyanobacteria, was found in the monsoon soil due to continuous flooding in the field. Cyanobacteria participate in soil N-cycle dynamics and that allows the growth of another phylum, the Nitrospirae. Both of these phyla were in high abundance in the monsoon soils as found from the metagenomics analysis. Ammonia production under water logging promotes the dominance of the Nitrospirae(Vlek and Craswell, 1981) while further conversion to nitrite enhances Cyanobacterial growth. Alpha-proteobacteria can participate in diverse soil activities due to their variable metabolic abilities like mineralization, metal mobilization by changing the soil redox status, methanogenesis etc. The plethora of *Gemmata*sp. and *Pirllula* sp. that comes under the phylum Plactomycetes, were higher in the pre-monsoon milking soil phase due to their aerobic chemoheterotrophic metabolism. During this phase, water application was ceased resulting aerobic soil status. The highly abundant genus DA101 of phylum Verrucomicrobia was found to be more dominant in developing soil compare to the milking or harvesting soils, although its proper assessment and role in environmental ecology is still unclear except that these microbes participate in geochemical cycling in soils. The microbial distribution and inter-connectivity were found to be influenced by or linked to the differential distribution of elements in soil. Chloflexi, Proteobacteria, Planctomycetes, Acidobacteria, Cyanobacteria, Verrucomicrobia, Actinobacteria and Bacteroidetes are the main influencers in the observed

microbial network analysis where these microbial groups are in the centre of the distribution, their influence branching out to other microbial groups. The network pattern was similar in the developing and milking phase soils but was changed in the harvesting phase. A large part of this metagenomics data revealed the crucial role of unidentified microbes in nutrient cycling as well as inter-microbial community interactions, but their probable mechanism remains uncertain.

Some earlier studies reported that the very high water-holding capacity of soil (i.e. monsoon condition) can result in a continual decrease in the total N mineralization compared to the 50-70% water content soil or the re-watering process(Denef et al., 2001; Chen et al., 2012). After re-watering of the paddy soil, aerobic microbes consume the oxygen present and the stagnant anoxic condition triggers other anaerobic or facultative microbes to use other electron acceptors present in the soil like nitrate, Mn(IV), Fe(III), SO_4^{2-} and CO_2, respectively(Liesack et al., 2000). Verrucomicrobia and rice field archaea are predominant in the monsoon soil, influencing the polysaccharolysis and methanogenesis in soil(Schütz et al., 1989; Janssen et al., 1997). In anoxic soil, oxygen-independent Fe oxidation process occurs by nitrate utilizing Fe-oxidizer microbes (Ratering and Schnell, 2000). In soil, the bioavailable content of P is also less (around 0.05% of the total P available in soil) and many species of free-living bacteria, endophytic bacteria and actinobacteria convert that unavailable fraction of organic P to phyto-available forms(Adhya et al., 2015). Microbial dissolution of K from mineral complexes is generally performed by several rhizobacterial groups including several species of *Bacillus* sp., *Acidothobacillus* sp., *Pseudomonas* sp., *Rhizobium* sp., *Burkholderia* sp.(Sattar et al., 2019), that are mostly predominate in the pre-monsoon cycling soil. Incremental release of soil Ca and Mg under pre-monsoon soil compared to the monsoon soil has been observed in this study, which also might result from additional microbial mineralization. Microbial mineralization of Ca in soil was found to increase in the presence of more available Mg(Chen et al., 2018). Based on previous reports and the findings from this present study, it must be emphasized that the combined effect of drying-wetting cycles of irrigation can help maintain a thriving soil microbial community that in turn can influence the availability of soil nutrients in the plant rhizosphere. This field study showed the increased total and bioavailable concentrations of nutrients in pre-monsoon soil was due to the frequent change in soil physico-chemical parameters when compared with conventional stagnant monsoon irrigated soil. This correlative research has established the role of different microbial phyla in the release of nutrient pulses under the pre-monsoon soil cycles providing higher bioavailability to the crop.

Therefore, the pre-monsoon drying-wetting cycle of field management and microbial activities can release nutrients in a more bioavailable form while compared to the conventional monsoon irrigation process.

Concluding remarks

In conclusion it can be stated that rice cultivation under pre-monsoon drying-wetting irrigation has been proven to be efficient which further found to be effective in modulating soil biota. This field study showed the increased total and bioavailable concentrations of nutrients in pre-monsoon soil at all the three plant growth phases, was due to the frequent change in soil physico-chemical parameters compared to the conventional monsoon soil. Cultivated rice plant uptake of total nutrients was measured higher in pre-monsoonal cultivation at all the three growth phases- developing, milking and harvest than the monsoonal cultivations. Cycling of water stagnancy, release and re-watering during the pre-monsoon season was found useful in loosing the bulk nutrients from the soil minerals, increasing the plant nutrient quality as we as the microbial biomass load in the soil than the prolonged waterlog during the monsoonal season causing flushed out the surface nutrient content and less microbial biomass load. Natural soil microbial diversity has been counted with their species richness in these respective soils with greater activity and diversity observed by metagenomics analysis in the pre-monsoon soil with highest richness at the harvest phase. With further correlative research, the role of different microbial phyla in the release of nutritional pulses under the pre-monsoon soil with higher bioavailability to the plant system has been established. Hence, a combinatory effect of pre-monsoon field management and microbial activities in releasing nutritional elements in a more bioavailable form compared to the conventional monsoon cultivation process has been proven.

Acknowledgment

The authors are thankful to IISER-K for providing infrastructure as well as core facilities (XRF DST-FIST laboratory). The authors are also thankful to BHU lab facilities. AM is thankful to the Ministry of Earth Sciences, India (MoES/P.O. (Geosci)/56/2015) for providing JRF and IISER Kolkata for providing SRF. Bulk of the fellowship amount to AM has been used in research expenses. MKU is thankful to the Council of Scientific and Industrial Research (CSIR) for CSIR-SRF (09/013(0853)/2018-EMR-I). PKD is thankful for UGC-SRF. Authors are also thankful to

Genotypic Technology [P] Ltd., Bangalore, India for the metagenomics analysis. Authors are cordially thankful to Prof. Anthony J. Miller, John Innes Centre, Norwich UK for his unconditional support in form of thorough revision of this manuscript.

Authors Credit

AM conceptualized the idea; AM performed field works, lab experiments and manuscript writing; MKU performed partial lab work and manuscript writing; PKD interpreted analysed dataset and contributed in revising manuscript; BG performed XRF analysis and manuscript writing; SS, and AKS revised and finalized the manuscript.

Authors would also like to thank Mr. Kedarnath Majumdar, landowner who selflessly helped with the field set up and management during this long-term experiment.

Conflict of interest

Authors declare that there is no conflict of interest.

References

Adhya, T.K., N. Kumar, G. Reddy, A.R. Podile, H. Bee, et al. 2015. Microbial mobilization of soil phosphorus and sustainable P management in agricultural soils. Curr. Sci. 108(7): 1280–1287. doi: 10.18520/cs/v108/i7/1280-1287.

Afsal, F., A. Majumdar, J.S. Kumar, and S. Bose. 2020. Microbial Inoculation to Alleviate the Metal Toxicity in Crop Plants and Subsequent Growth Promotion. Sustain. Solut. Elem. Defic. Excess Crop Plants: 451–479. doi: 10.1007/978-981-15-8636-1_17.

Baldwin, D.S., and A.M. Mitchell. 2000. The effects of drying and re-flooding on the sediment and soil nutrient dynamics of lowland river-floodplain systems: A synthesis. River Res. Appl. 16(5): 457–467. doi: 10.1002/1099-1646(200009/10)16:5<457::aid-rrr597>3.0.co;2-b.

Bickel, S., and D. Or. 2020. Soil bacterial diversity mediated by microscale aqueous-phase processes across biomes. Nat. Commun. 11(1): 1–9.

Birch, H.F. 1958. The effect of soil drying on humus decomposition and nitrogen availability. Plant Soil 10(1): 9–31. doi: 10.1007/BF01343734.

Blackwell, M.S.A., P.C. Brookes, N. de la Fuente-Martinez, H. Gordon, P.J. Murray, et al. 2010. Phosphorus Solubilization and Potential Transfer to Surface Waters from the Soil Microbial Biomass Following Drying–Rewetting and Freezing–Thawing. 1st ed. Elsevier Inc.

Bünemann, E.K., B. Keller, D. Hoop, K. Jud, P. Boivin, et al. 2013. Increased availability of phosphorus after drying and rewetting of a grassland soil: processes and plant use. Plant Soil 370(1): 511–526.

Chen, Y., R. Liu, C. Sun, P. Zhang, C. Feng, et al. 2012. Spatial and temporal variations in nitrogen and phosphorous nutrients in the Yangtze River Estuary. Mar. Pollut. Bull. 64(10): 2083–2089.

Chen, T., P. Shi, Y. Li, T. Duan, Y. Yu, et al. 2018. Biomineralization of varied calcium carbonate crystals by the synergistic effect of silk fibroin/magnesium ions in a microbial system. CrystEngComm 20(17): 2366–2373.

Dangar, S., A. Asoka, and V. Mishra. 2021. Causes and implications of groundwater depletion in India: A review. J. Hydrol. 596: 126103.

Delgado-Baquerizo, M., F.T. Maestre, P.B. Reich, T.C. Jeffries, J.J. Gaitan, et al. 2016. Microbial diversity drives multifunctionality in terrestrial ecosystems. Nat. Commun. 7(1): 1–8.

Denef, K., J. Six, H. Bossuyt, S.D. Frey, E.T. Elliott, et al. 2001. Influence of dry–wet cycles on the interrelationship between aggregate, particulate organic matter, and microbial community dynamics. Soil Biol. Biochem. 33(12–13): 1599–1611.

Dodd, I.C., J. Puértolas, K. Huber, J.G. Pérez-Pérez, H.R. Wright, et al. 2015. The importance of soil drying and re-wetting in crop phytohormonal and nutritional responses to deficit irrigation. J. Exp. Bot. 66(8): 2239–2252. doi: 10.1093/jxb/eru532.

Dubey, P.K., G.S. Singh, and P.C. Abhilash. 2020. Agriculture in a changing climate. Adaptive Agricultural Practices. Springer. p. 1–10

523 Dubey, P.K., A. Singh, R. Chaurasia, K.K. Pandey, A.K. Bundela, et al. 2021a. Planet friendly
524 agriculture: Farming for people and the planet. Curr. Res. Environ. Sustain. 3: 100041.

525 Dubey, P.K., A. Singh, R. Chaurasia, K.K. Pandey, A.K. Bundela, et al. 2022. Animal manures
526 and plant residue-based amendments for sustainable rice-wheat production and soil fertility
527 improvement in eastern Uttar Pradesh, North India. Ecol. Eng. 177: 106551.

528 Dubey, P.K., A. Singh, R. Chaurasia, K.K. Pandey, and S. Singh. 2021b. Fostering Nature-Based
529 Solutions for Ecorestoration and Attaining United Nations Sustainable Development Goals.

530 Fageria, N.K., V.C. Baligar, and C.A. Jones. 2010. Growth and mineral nutrition of field crops.
531 CRC Press.

532 Gupta, R.S. 2013. Molecular markers for photosynthetic bacteria and insights into the origin and
533 spread of photosynthesis. Adv. Bot. Res. 66: 37–66.

534 Gupta, A., A. Majumdar, and S. Srivastava. 2022. Approaches for assisted phytoremediation of
535 arsenic contaminated sites. Assisted Phytoremediation. Elsevier. p. 221–242

536 Hasanuzzaman, M., K. Nahar, and M. Fujita. 2018. Mechanisms of arsenic toxicity and tolerance
537 in plants. Mech. Arsen. Toxic. Toler. Plants (November): 1–508. doi: 10.1007/978-981-13-
538 1292-2.

539 Heuck, C., A. Weig, and M. Spohn. 2015. Soil microbial biomass C: N: P stoichiometry and
540 microbial use of organic phosphorus. Soil Biol. Biochem. 85: 119–129.

541 Huang, Z., E.L. Nya, M.A. Rahman, T.B. Mwamila, V. Cao, et al. 2021. Integrated water
542 resource management: Rethinking the contribution of rainwater harvesting. Sustainability
543 13(15): 8338.

544 Janssen, P.H., A. Schuhmann, E. Mörschel, and F.A. Rainey. 1997. Novel anaerobic
545 ultramicrobacteria belonging to the Verrucomicrobiales lineage of bacterial descent isolated
546 by dilution culture from anoxic rice paddy soil. Appl. Environ. Microbiol. 63(4): 1382–
547 1388.

548 Jia, R., K. Wang, L. Li, Z. Qu, W. Shen, et al. 2020. Abundance and community succession of

549 nitrogen-fixing bacteria in ferrihydrite enriched cultures of paddy soils is closely related to
550 Fe (III)-reduction. Sci. Total Environ. 720: 137633.

551 Johannesson, K.H., and K. Neumann. 2013. Geochemical cycling of mercury in a deep, confined
552 aquifer: Insights from biogeochemical reactive transport modeling. Geochim. Cosmochim.
553 Acta 106: 25–43.

554 Kabata-Pendias, A. 2000. Trace elements in soils and plants. CRC press.

555 Kielak, A.M., C.C. Barreto, G.A. Kowalchuk, J.A. van Veen, and E.E. Kuramae. 2016. The
556 ecology of Acidobacteria: moving beyond genes and genomes. Front. Microbiol. 7: 744.

557 Kumarathilaka, P., S. Seneweera, A. Meharg, and J. Bundschuh. 2018. Arsenic speciation
558 dynamics in paddy rice soil-water environment: sources, physico-chemical, and biological
559 factors-a review. Water Res. 140: 403–414.

560 Laha, M., H. Arambagh, and W. Bengal. 2013. Social Implication of Arsenic Pollution in
561 Eastern Barddhaman. Transactions 35(2): 173–184.

562 Leita, L., M. De Nobili, C. Mondini, G. Muhlbachova, L. Marchiol, et al. 1999. Influence of
563 inorganic and organic fertilization on soil microbial biomass, metabolic quotient and heavy
564 metal bioavailability. Biol. Fertil. Soils 28(4): 371–376.

565 Liesack, W., S. Schnell, and N.P. Revsbech. 2000. Microbiology of flooded rice paddies. FEMS
566 Microbiol. Rev. 24(5): 625–645. doi: 10.1016/S0168-6445(00)00050-4.

567 Lu, T., Y. Wang, H. Zhu, X. Wei, and M. Shao. 2020. Drying-wetting cycles consistently
568 increase net nitrogen mineralization in 25 agricultural soils across intensity and number of
569 drying-wetting cycles. Sci. Total Environ. 710: 135574.

570 Majumdar, A. 2021. Arsenic Bio-regulation Management and Altered Plant Physiology under
571 Different Irrigation Regime.

572 Majumdar, A., A. Barla, M.K. Upadhyay, D. Ghosh, P. Chaudhuri, et al. 2018.
573 Vermiremediation of metal(loid)s via Eichornia crassipes phytomass extraction: A
574 sustainable technique for plant amelioration. J. Environ. Manage. 220(May): 118–125. doi:

575 10.1016/j.jenvman.2018.05.017.

576 Majumdar, A., and S. Bose. 2017. Toxicogenesis and metabolism of arsenic in rice and wheat
577 plants with probable mitigation strategies. Arsen. Risks Expo. Behav. Environ. Toxicol.:
578 149–166.

579 Majumdar, A., and S. Bose. 2018. A glimpse on uptake kinetics and molecular responses of
580 arsenic tolerance in Rice plants. Mechanisms of arsenic toxicity and tolerance in plants.
581 Springer. p. 299–315

582 Majumdar, A., J.S. Kumar, Sheena, and S. Bose. 2020a. Agricultural Water Management
583 Practices and Environmental Influences on Arsenic Dynamics in Rice Field. Arsen. Drink.
584 Water Food: 425–443. doi: 10.1007/978-981-13-8587-2_17.

585 Majumdar, A., A. Shrivastava, S.R. Sarkar, S. Sathyavelu, A. Barla, et al. 2020b. Hydrology,
586 sedimentation and mineralisation: A wetland ecology perspective. Clim. Chang. Environ.
587 Sustain. 8(2): 134–151.

588 Majumdar, A., M.K. Upadhyay, B. Giri, S. Srivastava, A.K. Srivastava, et al. 2021. Arsenic
589 dynamics and flux assessment under drying-wetting irrigation and enhanced microbial
590 diversity in paddy soils: A four year study in Bengal delta plain. J. Hazard. Mater.
591 409(November): 124443. doi: 10.1016/j.jhazmat.2020.124443.

592 Majumdar, A., M.K. Upadhyay, J.S. Kumar, Sheena, A. Barla, et al. 2019. Ultra-structure
593 alteration via enhanced silicon uptake in arsenic stressed rice cultivars under intermittent
594 irrigation practices in Bengal delta basin. Ecotoxicol. Environ. Saf. 180(May): 770–779.
595 doi: 10.1016/j.ecoenv.2019.05.028.

596 Majumdar, A., M.K. Upadhyay, M. Ojha, F. Afsal, B. Giri, et al. 2022. Enhanced
597 phytoremediation of Metal (loid) s via spiked ZVI nanoparticles: An urban clean-up
598 strategy with ornamental plants. Chemosphere 288: 132588.

599 Mikha, M.M., C.W. Rice, and G.A. Milliken. 2005. Carbon and nitrogen mineralization as
600 affected by drying and wetting cycles. Soil Biol. Biochem. 37(2): 339–347. doi:
601 10.1016/j.soilbio.2004.08.003.

602 Miller, A.E., J.P. Schimel, T. Meixner, J.O. Sickman, and J.M. Melack. 2005. Episodic rewetting
603 enhances carbon and nitrogen release from chaparral soils. Soil Biol. Biochem. 37(12):
604 2195–2204.

605 Mooshammer, M., F. Hofhansl, A.H. Frank, W. Wanek, I. Hämmerle, et al. 2017. Decoupling of
606 microbial carbon, nitrogen, and phosphorus cycling in response to extreme temperature
607 events. Sci. Adv. 3(5): 1–14. doi: 10.1126/sciadv.1602781.

608 Mukherji, A. 2007. The energy-irrigation nexus and its impact on groundwater markets in
609 eastern Indo-Gangetic basin: Evidence from West Bengal, India. Energy Policy 35(12):
610 6413–6430.

611 Nickson, R.T., J.M. McArthur, P. Ravenscroft, W.G. Burgess, and K.M. Ahmed. 2000.
612 Mechanism of arsenic release to groundwater, Bangladesh and West Bengal. Appl.
613 geochemistry 15(4): 403–413.

614 Nishio, T., H. Sekiya, K. Toriyama, and K. Kogano. 1994. Changes in gross rates of nitrogen
615 transformations in soil caused by conversion of paddy fields to upland fields. Soil Sci. Plant
616 Nutr. 40(2): 301–309.

617 Ondov, B.D., N.H. Bergman, and A.M. Phillippy. 2011. Interactive metagenomic visualization in
618 a Web browser. BMC Bioinformatics 12(1): 385. doi: 10.1186/1471-2105-12-385.

619 Parmar, P., and S.S. Sindhu. 2013. Potassium Solubilization by Rhizosphere Bacteria: Influence
620 of Nutritional and Environmental Conditions. J. Microbiol. Res. 3(1): 25–31. doi:
621 10.5923/j.microbiology.20130301.04.

622 Pearson, K.A., G.M. Millar, G.J. Norton, and A.H. Price. 2018. Alternate wetting and drying in
623 Bangladesh: Water-saving farming practice and the socioeconomic barriers to its adoption.
624 Food Energy Secur. 7(4): 1–12. doi: 10.1002/fes3.149.

625 Ramette, A. 2007. Multivariate analyses in microbial ecology. FEMS Microbiol. Ecol. 62(2):
626 142–160. doi: 10.1111/j.1574-6941.2007.00375.x.

627 Ratering, S., and S. Schnell. 2000. Localization of iron-reducing activity in paddy soilby profile
628 studies. Biogeochemistry 48(3): 341–365.

629 Ray Sarkar, S., A. Majumdar, A. Barla, N. Pradhan, S. Singh, et al. 2017. A conjugative study of
630 Typha latifolia for expunge of phyto-available heavy metals in fly ash ameliorated soil.
631 Geoderma 305(November): 354–362. doi: 10.1016/j.geoderma.2017.06.022.

632 Sattar, A., M. Naveed, M. Ali, Z.A. Zahir, S.M. Nadeem, et al. 2019. Perspectives of potassium
633 solubilizing microbes in sustainable food production system: A review. Appl. Soil Ecol.
634 133(July): 146–159. doi: 10.1016/j.apsoil.2018.09.012.

635 Schütz, H., W. Seiler, and R. Conrad. 1989. Processes involved in formation and emission of
636 methane in rice paddies. Biogeochemistry 7(1): 33–53.

637 Shrivastava, A., A. Barla, A. Majumdar, S. Singh, and S. Bose. 2020. Arsenic mitigation in rice
638 grain loading via alternative irrigation by proposed water management practices.
639 Chemosphere 238: 124988. doi: 10.1016/j.chemosphere.2019.124988.

640 Shrivastava, A., A. Barla, H. Yadav, and S. Bose. 2014. Arsenic contamination in shallow
641 groundwater and agricultural soil of Chakdaha block, West Bengal, India. Front. Environ.
642 Sci. 2: 50.

643 Song, T., D. Das, Q. Hu, F. Yang, and J. Zhang. 2021. Alternate wetting and drying irrigation
644 and phosphorus rates affect grain yield and quality and heavy metal accumulation in rice.
645 Sci. Total Environ. 752: 141862.

646 Surendran, U., P. Raja, M. Jayakumar, and S.R. Subramoniam. 2021. Use of efficient water
647 saving techniques for production of rice in India under climate change scenario: A critical
648 review. J. Clean. Prod. 309: 127272.

649 Tulip, S.S., M.S. Siddik, M.N. Islam, A. Rahman, A.T. Haghighi, et al. 2022. The impact of
650 irrigation return flow on seasonal groundwater recharge in northwestern Bangladesh. Agric.
651 Water Manag. 266: 107593.

652 Upadhyay, M.K., A. Majumdar, A. Barla, S. Bose, and S. Srivastava. 2021. Thiourea
653 supplementation mediated reduction of grain arsenic in rice (Oryza sativa L.) cultivars: A
654 two year field study. J. Hazard. Mater. 407(September 2020): 124368. doi:
655 10.1016/j.jhazmat.2020.124368.

Upadhyay, M.K., A. Majumdar, A.K. Srivastava, S. Bose, P. Suprasanna, et al. 2022. Antioxidant enzymes and transporter genes mediate arsenic stress reduction in rice (Oryza sativa L.) upon thiourea supplementation. Chemosphere 292: 133482.

Venterink, H.O., T.E. Davidsson, K. Kiehl, and L. Leonardson. 2002. Impact of drying and re-wetting on NPK dynamics in a wetland soil.pdf. : 119–130.

Vlek, P.L., and E.T. Craswell. 1981. Ammonia volatilization from flooded soils. Fertil. Res. 2(4): 227–245.

Walkley, A., and I.A. Black. 1934. An examination of the Degtjareff method for determining soil organic matter, and a proposed modification of the chromic acid titration method. Soil Sci. 37(1): 29–38.

Wang, Y., C.R. Jensen, and F. Liu. 2017. Nutritional responses to soil drying and rewetting cycles under partial root-zone drying irrigation. Agric. Water Manag. 179: 254–259. doi: 10.1016/j.agwat.2016.04.015.

Wang, J., F. Pan, J. Soininen, J. Heino, and J. Shen. 2016. Nutrient enrichment modifies temperature-biodiversity relationships in large-scale field experiments. Nat. Commun. 7(1): 1–9.

Wu, J., and P.C. Brookes. 2005. The proportional mineralisation of microbial biomass and organic matter caused by air-drying and rewetting of a grassland soil. Soil Biol. Biochem. 37(3): 507–515.

Xiang, S.-R., A. Doyle, P.A. Holden, and J.P. Schimel. 2008. Drying and rewetting effects on C and N mineralization and microbial activity in surface and subsurface California grassland soils. Soil Biol. Biochem. 40(9): 2281–2289.

Zhou, Z., C. Wang, and Y. Luo. 2020. Meta-analysis of the impacts of global change factors on soil microbial diversity and functionality. Nat. Commun. 11(1): 1–10.

Fig 1. Radar plot distribution of total soil elemental concentration in four consecutive years 2016-2019.

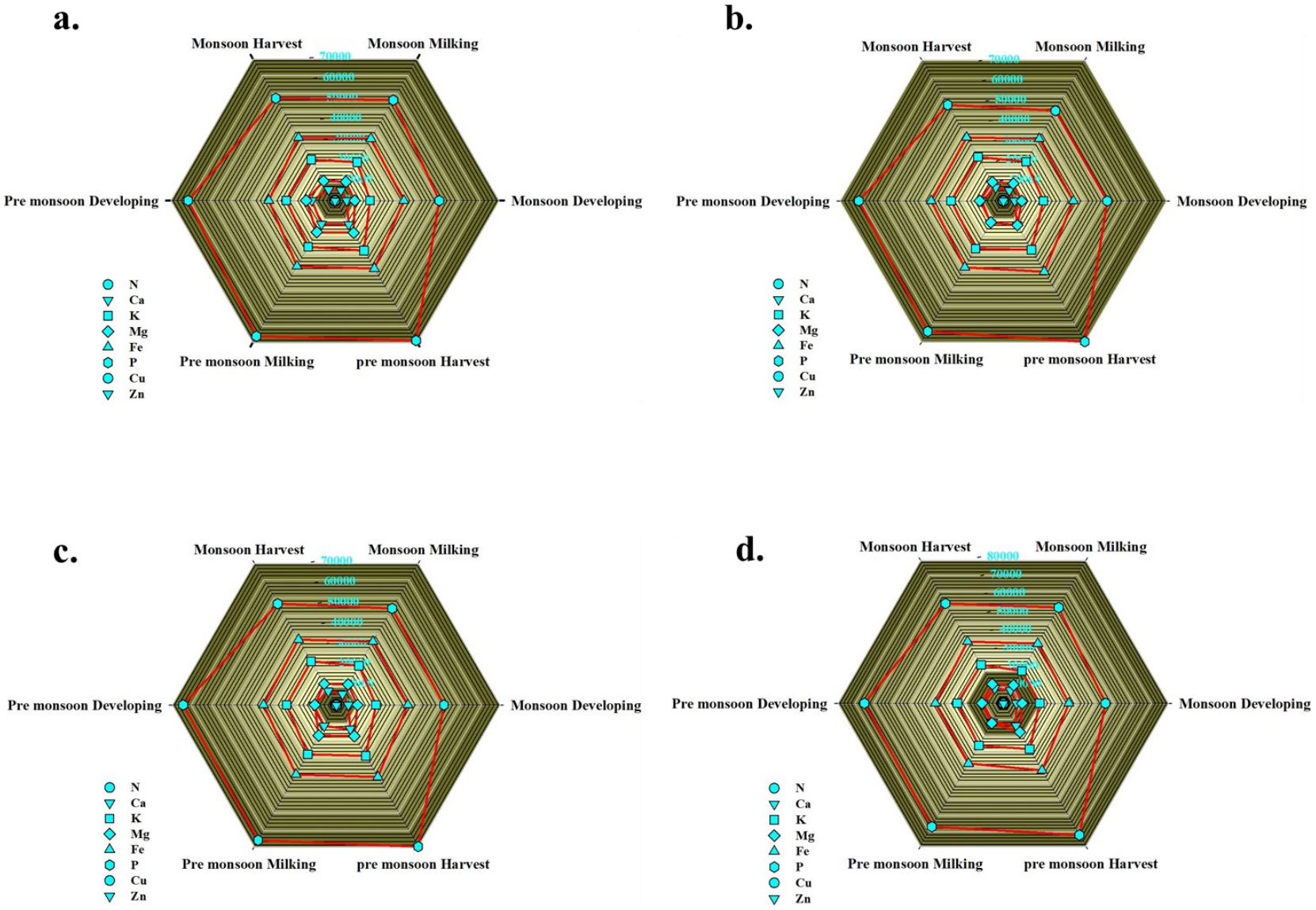

This radar plot shows a layered representation of element concentrations in two seasons with three sampling phases in four consecutive years from 2016 to 2019 under a same paddy field (**a-d**). This plot uses the average data of triplicated results. Radar plot shows the result in a centre-out form with lowest data at the core and the highest data at the verge. Dark grey colored lines inside the plot represents the minor grid that is sub-set of each data point. Major data range are mentioned with a gap of 10000 unit (unit = mg kg^{-1}) and sub set data gap represents 2000 unit each. This plot shows the concentration change of selected elements under field conditions with corresponding sub-set lines. From the graph, it can be seen that the pre-monsoonal soil contained highest amount of nutrients compared to the monsoonal soils. Data has been validated using one-way ANOVA ($p<0.05$) while plotting.

Fig 2. Element concentrations in whole rice plant (root+shoot) at three growth phases in four consecutive years.

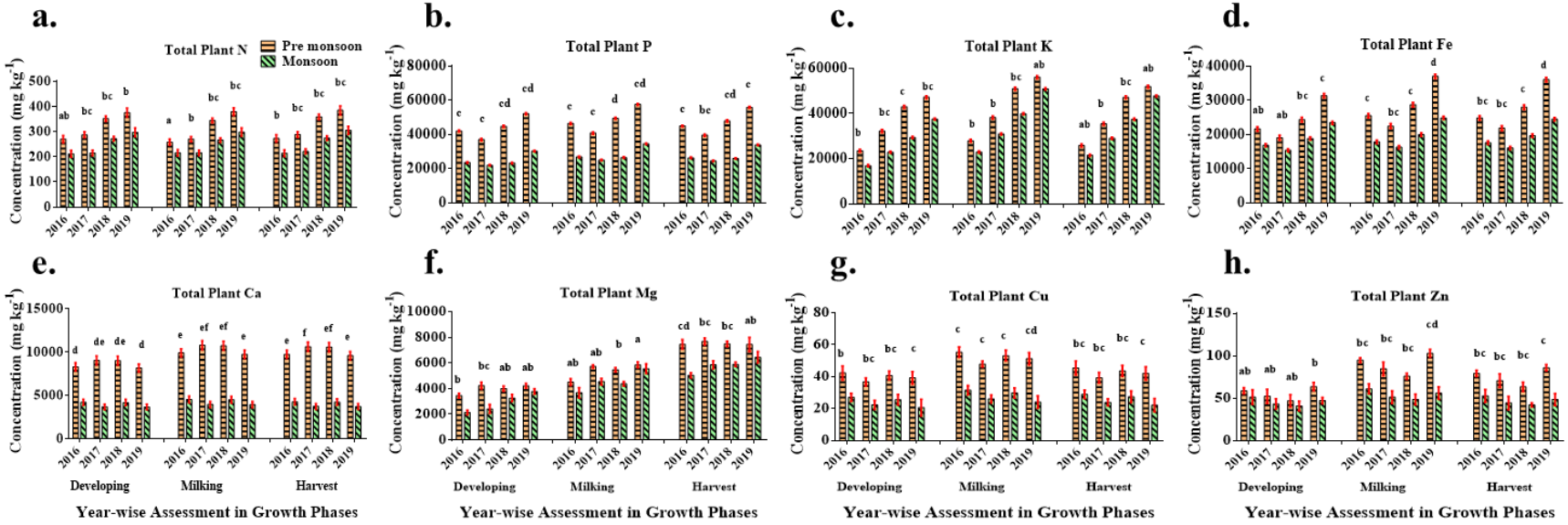

Rice plants grown in two different seasons accumulated differential concentrations of nutritional elements at three growth phases in four consecutive years from 2016 to 2019. Summed results of root and shoot analysis has been presented for a better assessment of element contents in whole rice plants. Selected elements concentration has been presented as a mean of triplicate data with standard deviation. One-way ANOVA ($p<0.05$) was used for data validation and for statistical differences in each data set, DMRT was used.

Fig 3. Correlation matrix plot of soil physico-chemical parameters and bioavailable nutritional elements in three phases and relative year-wise yield data.

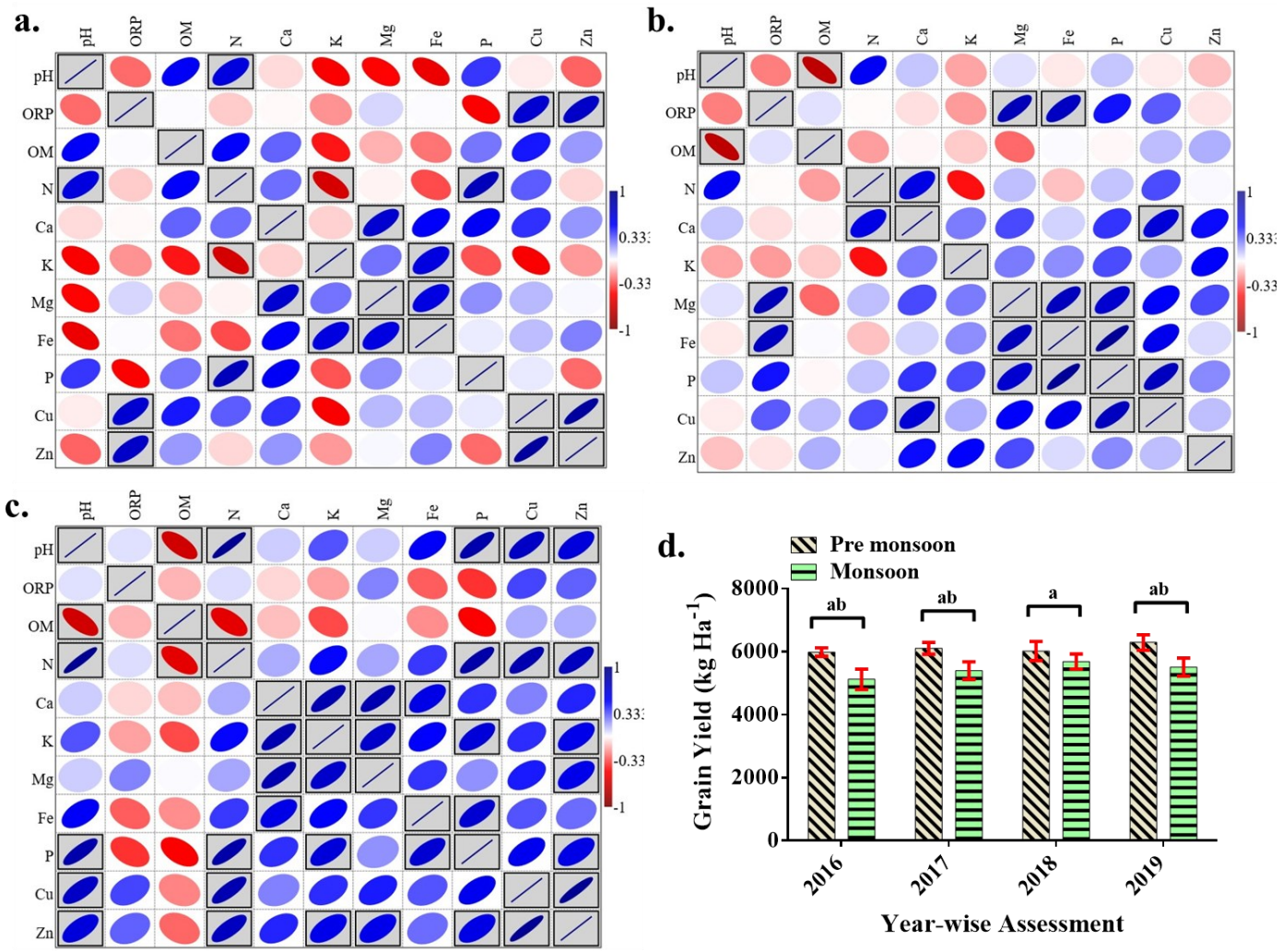

Soil physico-chemical parameters like pH, redox potential (ORP) and organic matter (OM) can influence bioavailability of soil elements. This figure represents the correlation matrix of bioavailable content of nutritional elements in soil with pH, ORP and OM under three different plant growth phases (a) developing, (b) milking and (c) harvest. All the data from four years are compared together to check the effect of plant growth phases on soil nutritional availability. Color code here represents a minimum (dark red) to maximum (violet) correlation whereas the sharpness in shape and direction of ovals also shows the degree of correlation. The more it is sharp, the more strongly correlated and upwards to downwards indicates either positive or negative relations. Grey colored shaded boxes indicates the $p<0.05$ significance results. The nutritional availability was found to be effective in yield enhancement as shown in (d) with yearly increment in the pre-monsoonal season. DMRT was used for statistical difference assessment.

Fig 4. Bioavailable concentration distribution of selected elements in field conditions under the influence of soil pH and microbial biomass.

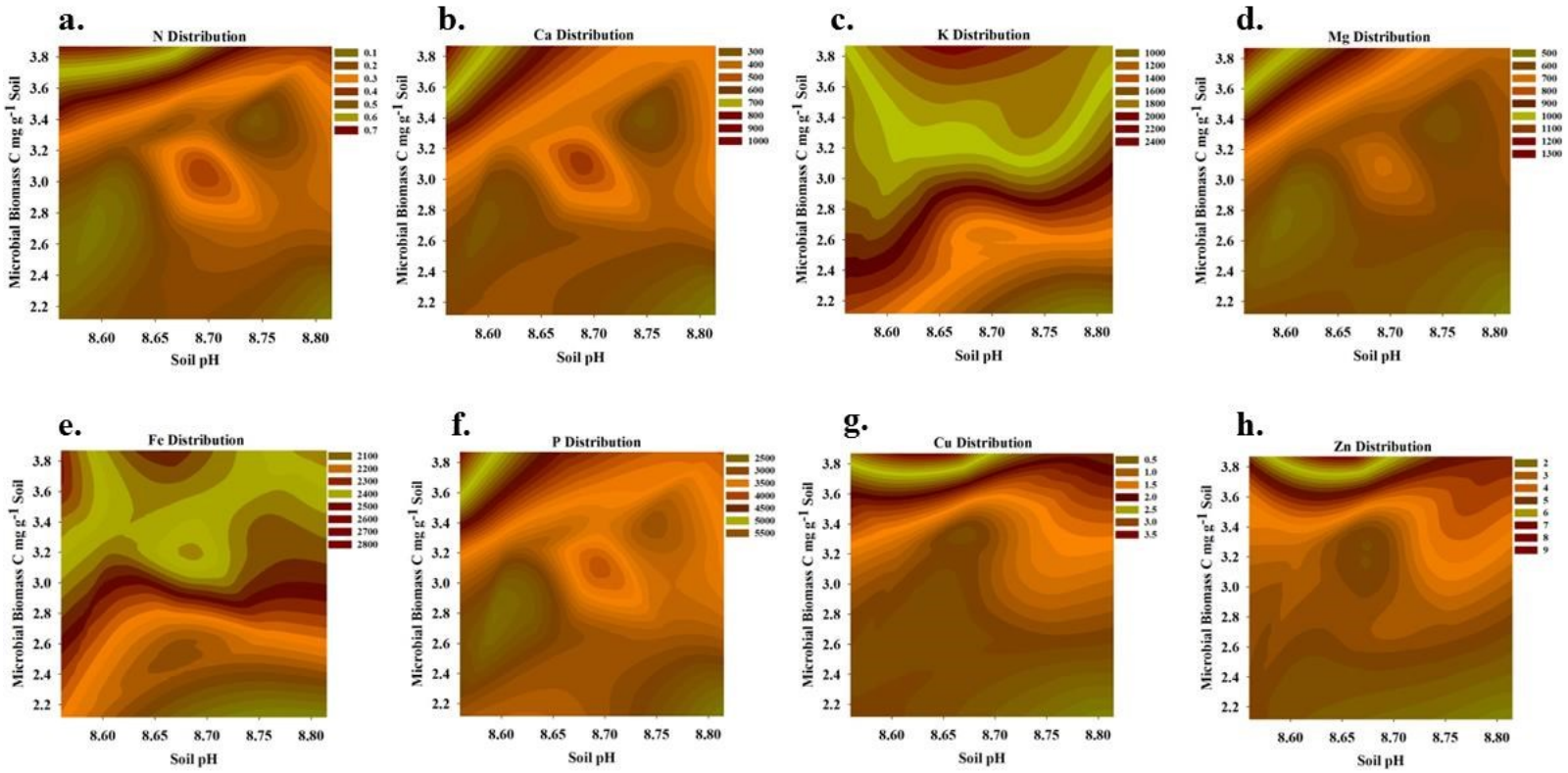

Bioavailability of crop nutritional elements are dispersive in nature and their distribution in the soil varies with active microbial biomass that in turn depends on soil pH. This contour map shows the soil pH and MBC of all the three phase soils together showing the pattern of elemental content distribution, getting changed with the other two. Due to the differential pH and MBC content in these soils, distribution of elements also gets changed. Each element has a different range of bioavailability and that has been represented in a colour code to understand the pattern of concentration distribution.

Fig 5. Principal component analysis of selected elements during three plant growth phases in four years (2016-2019).

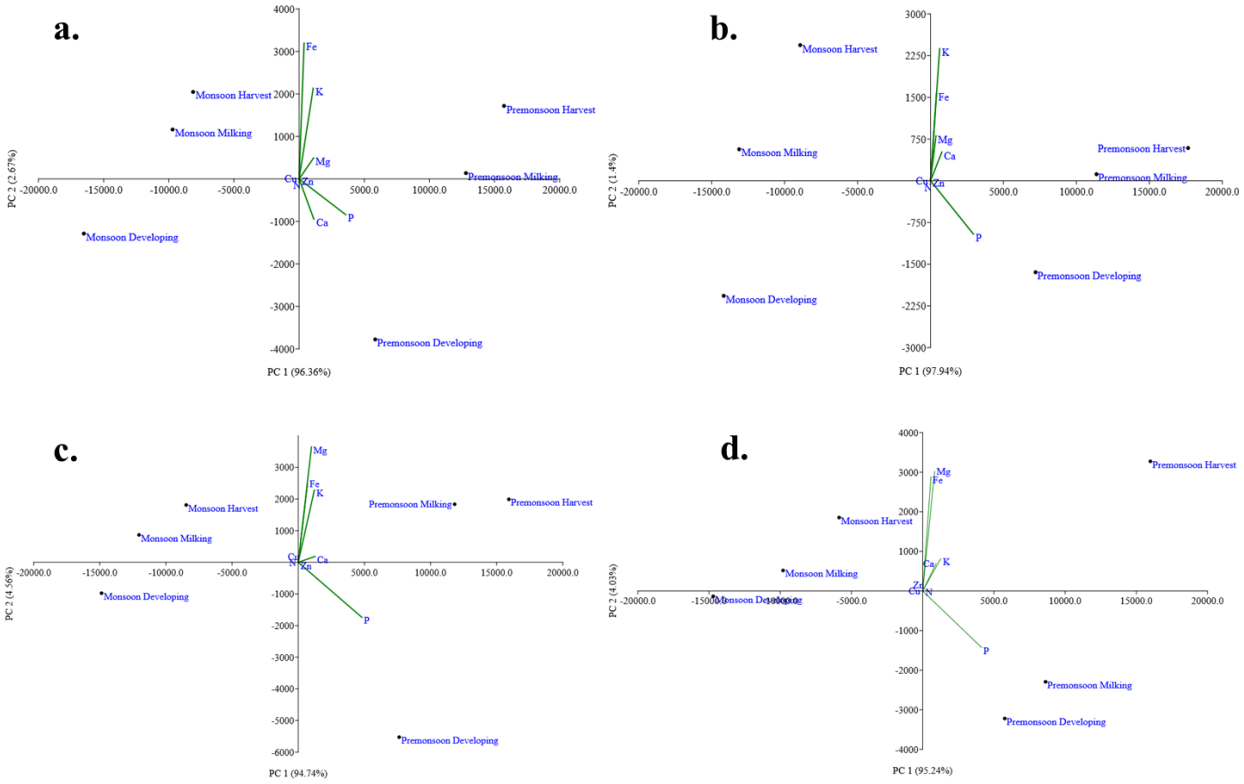

In four consecutive years 2016-2019 (**a-d**), the soil elements are differentially measured and found that all the soils have diverse content of elements and getting influenced under field conditions along with the plant growth phases. Among the analyzed components, first two components are presented here with variance % mentioned in parenthesis. Green lines are showing the bi-plot model in this multi-component analysis.

Fig 6. Krona chart of microbial diversity with relative abundance percent analysis of two seasonal soils at three growth phases.

a.

Developing

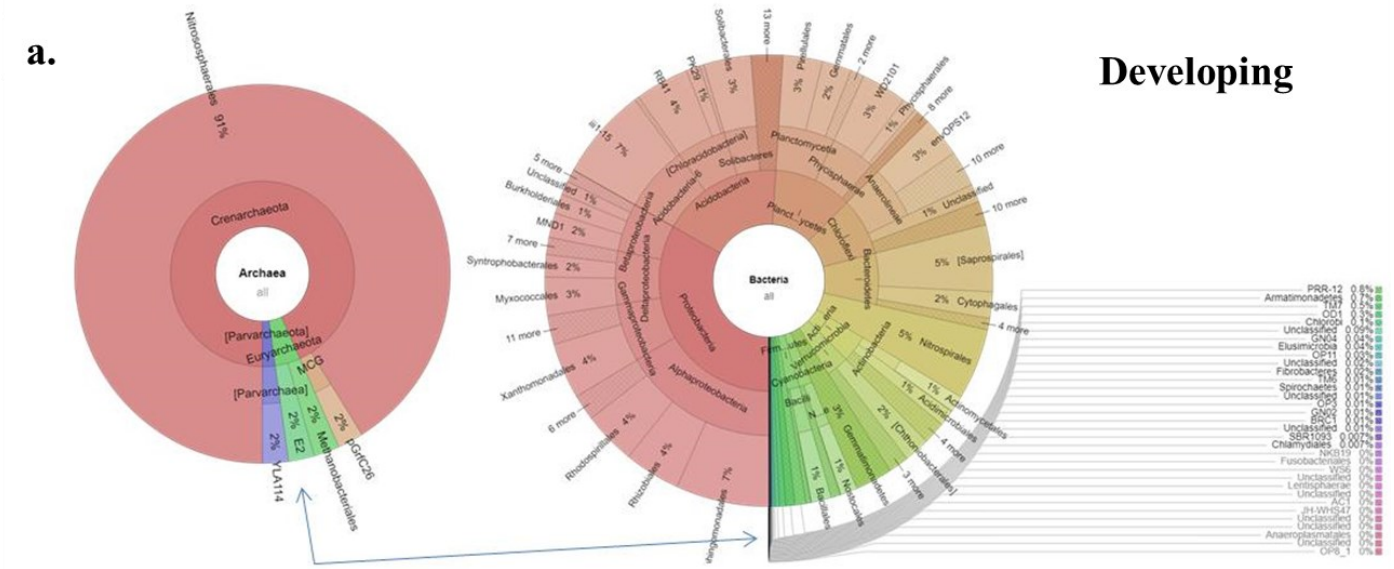

a1.

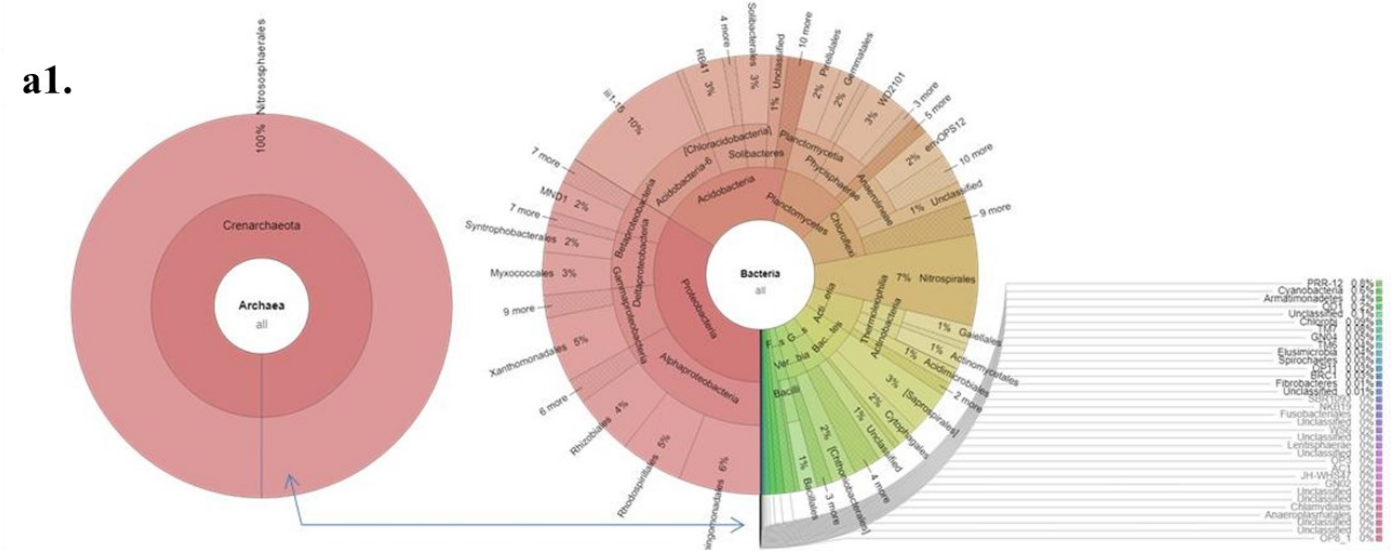

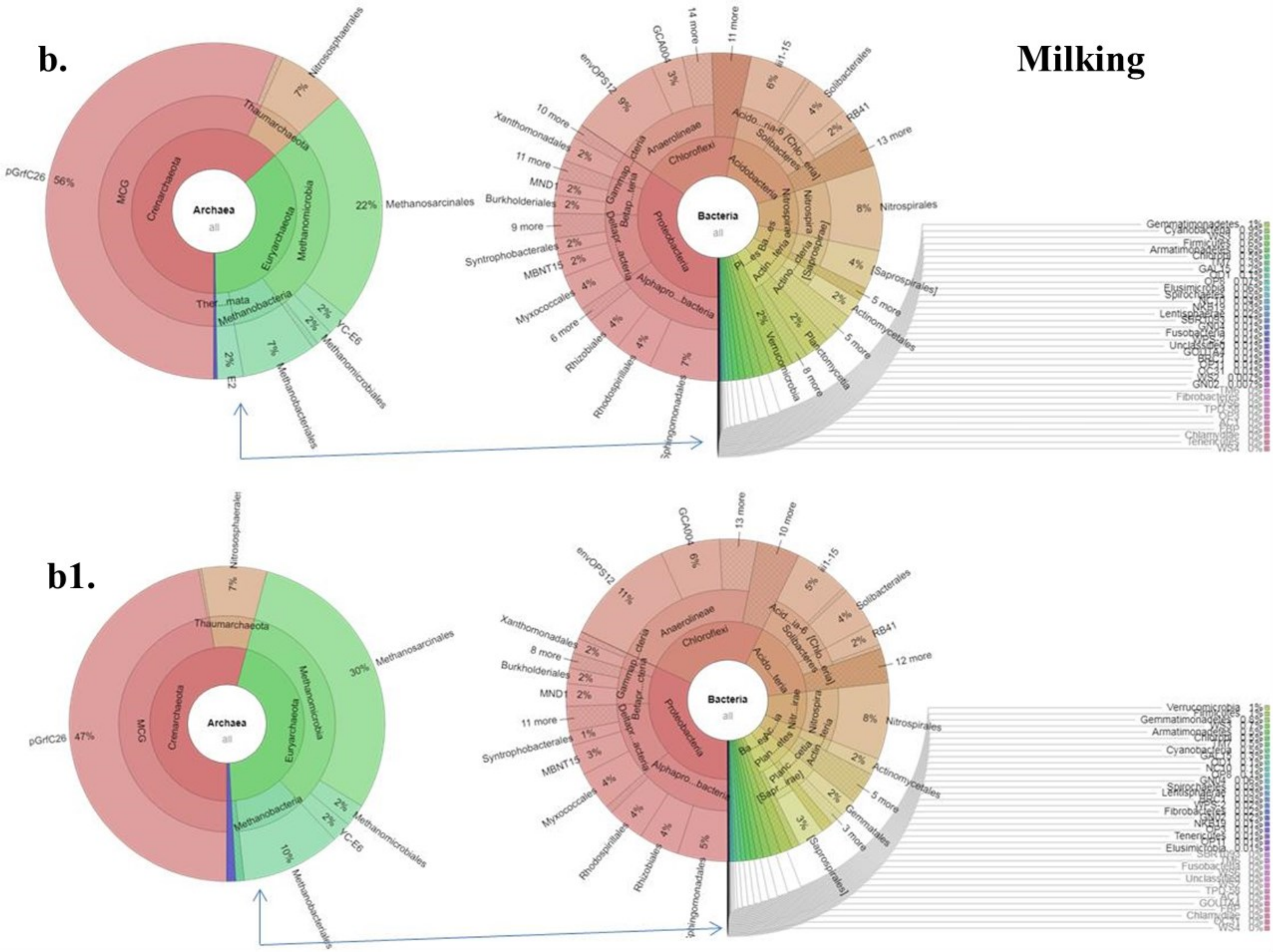
b.
Milking
b1.
Archaea
all
Bacteria
all
pGrfC26 56%
MCG
Crenarchaeota
Thaumarchaeota
Nitrososphaerales
7%
Euryarchaeota
Methanomicrobia
22% Methanosarcinales
Methanobacteria
Methanobacteriales
Methanomicrobiales
YC-E6
E2
Proteobacteria
Chloroflexi
Anaerolineae
Acidobacteria
Solibacteres
Nitrospirae
Nitrospira
8% Nitrospirales
Actinomycetales
Planctomycetia
Verrucomicrobia
[Saprospirales]
envOPS12
GCA004
Solibacterales
RB41
Xanthomonadales
Burkholderiales
MND1
Syntrophobacterales
MBNT15
Myxococcales
Rhizobiales
Rhodospirillales
Sphingomonadales
pGrfC26 47%
30% Methanosarcinales
10%
Gemmatales
Gemmatimonadetes
Cyanobacteria
Verrucomicrobia
Armatimonadetes
Fibrobacteres
Tenericutes
Elusimicrobia
Lentisphaerae
WS4

c.

Harvest

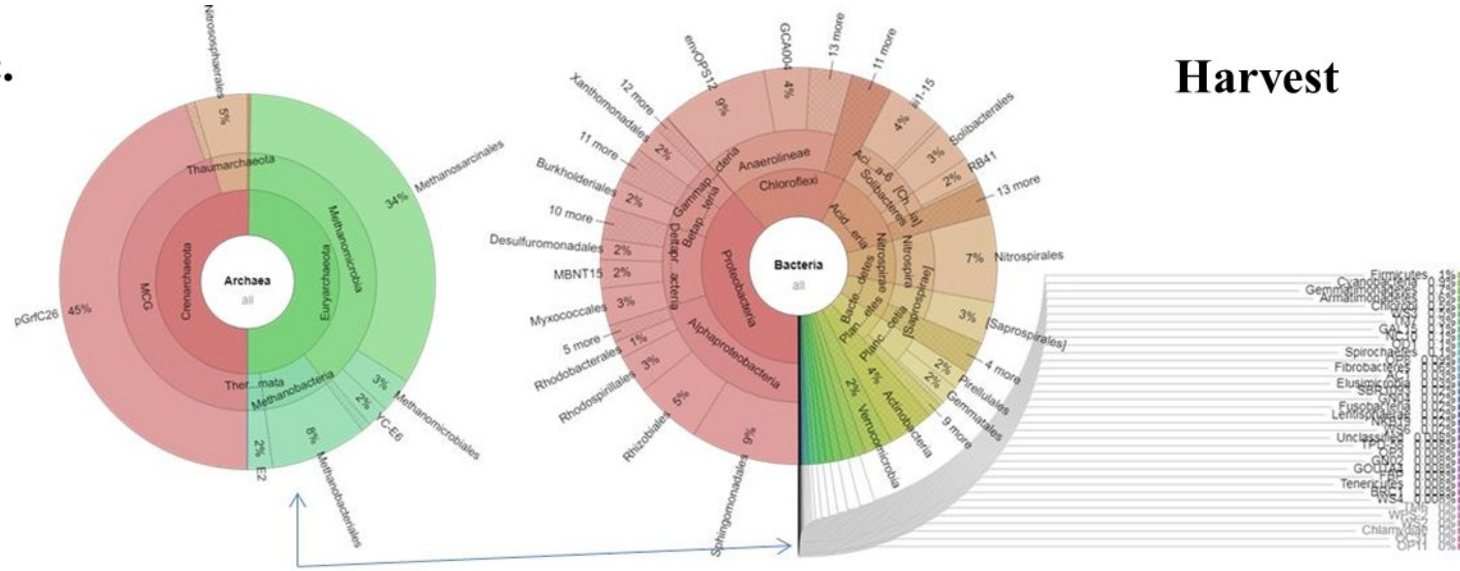
Archaea
all
Thaumarchaeota
Nitrososphaerales 5%
Crenarchaeota
MCG
pGrfC26 45%
Euryarchaeota
Methanomicrobia
34% Methanosarcinales
Methanobacteria
Ther...mata
3% Methanomicrobiales
2% YC-E6
8% Methanobacteriales
2% E2
Bacteria
all
Proteobacteria
Alphaproteobacteria
Chloroflexi
Anaerolineae
Nitrospirae
Nitrospira
7% Nitrospirales
3% [Saprospirales]
Actinobacteria
Verrucomicrobia
Gemmatales
Pirellulales
Solibacterales
RB41
envOPS12
GCA004
Xanthomonadales
Burkholderiales
Desulfuromonadales
MBNT15
Myxococcales
Rhodobacterales
Rhodospirillales
Rhizobiales
Sphingomonadales
Firmicutes
Spirochaetes
Fibrobacteres
Tenericutes
Chlamydiae
OP11

c1.

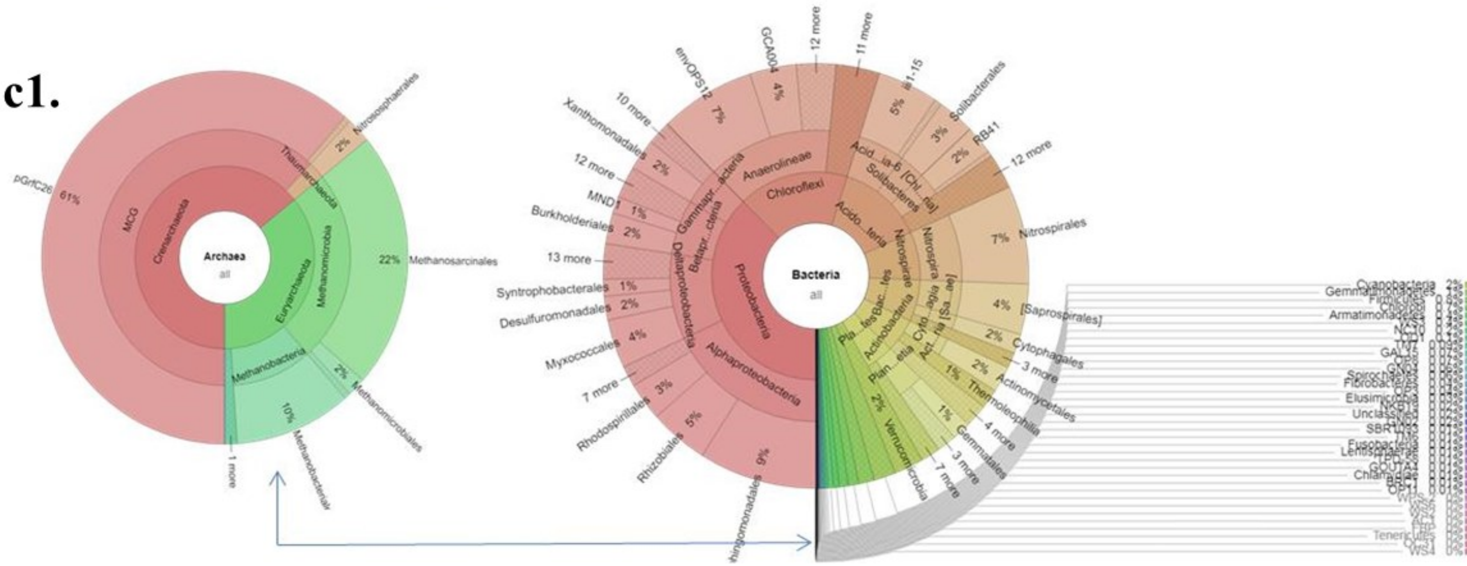
Archaea
all
pGrfC26 61%
MCG
Crenarchaeota
Thaumarchaeota
2% Nitrososphaerales
Euryarchaeota
Methanomicrobia
22% Methanosarcinales
Methanobacteria
2% Methanomicrobiales
10% Methanobacteriales
1 more
Bacteria
all
Proteobacteria
Alphaproteobacteria
Chloroflexi
Anaerolineae
Nitrospirae
Nitrospira
7% Nitrospirales
4% [Saprospirales]
2% Cytophagales
Actinomycetales
Thermoleophilia
Gemmatales
Verrucomicrobia
Solibacterales
RB41
envOPS12
GCA004
Xanthomonadales
MND1
Burkholderiales
Syntrophobacterales
Desulfuromonadales
Myxococcales
Rhodospirillales
Rhizobiales
Cyanobacteria
Armatimonadetes
Tenericutes
WS4

Krona interactive plot of microbial phylogenic classifications within each sample with occurrence percentages has been shown here. Developing (**a-a1**), milking (**b-b1**) and harvest (**c-c1**) phases soil samples were analysed using this krona plot where predominant bacterial and archaeal communities are represented in different shades of color. Samples from both pre-monsoonal (**a, b, c**) and monsoonal (**a1, b1, c1**) seasons have been considered for microbial diversity and abundance cross-check. The relative abundance of predominant microbial classes is presented here with mentioned percent obtained in the metagenomics analysis.

Fig 7. Microbial network analysis of three growth phase soils under influence of elemental content in pre-monsoonal and monsoonal seasons.

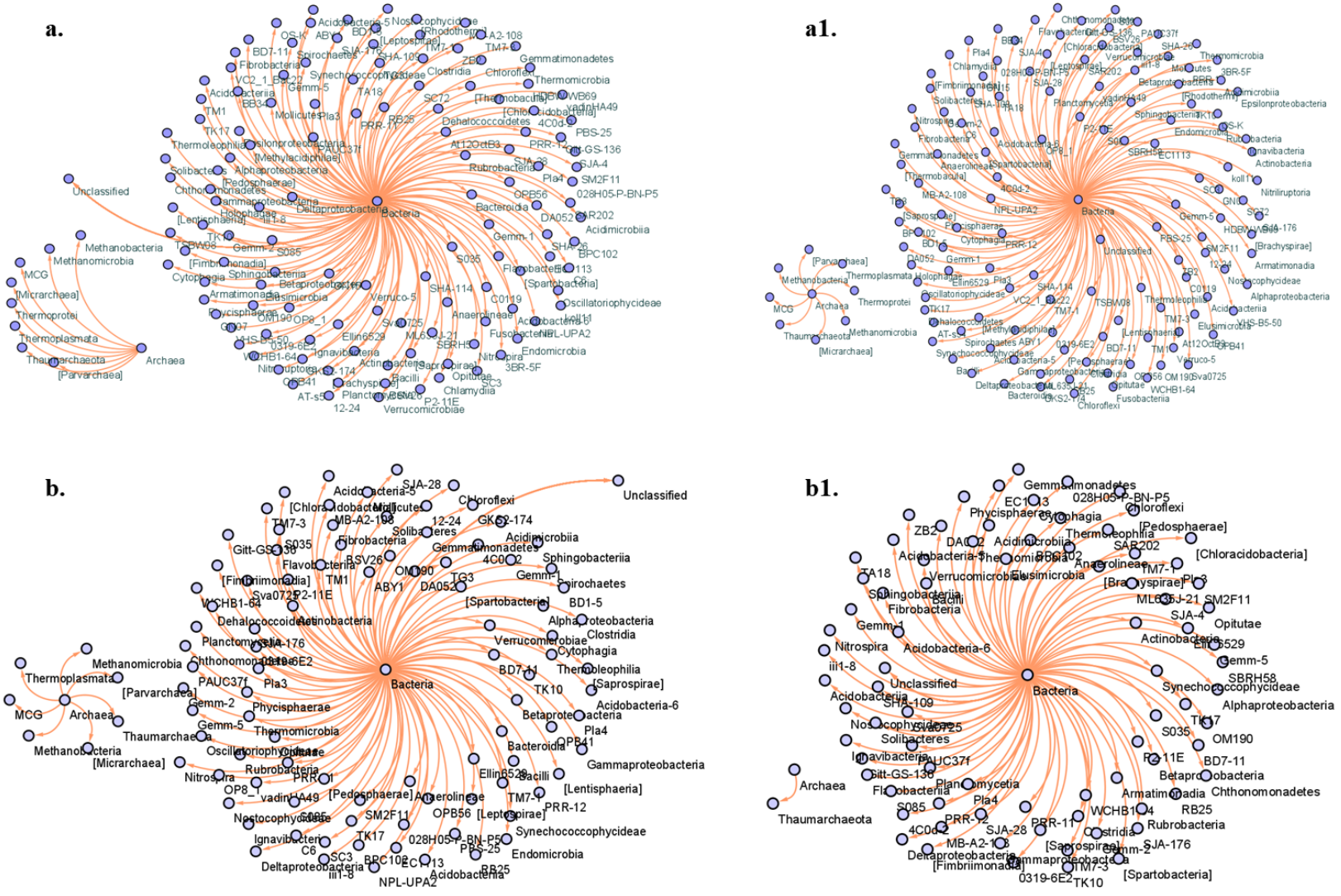

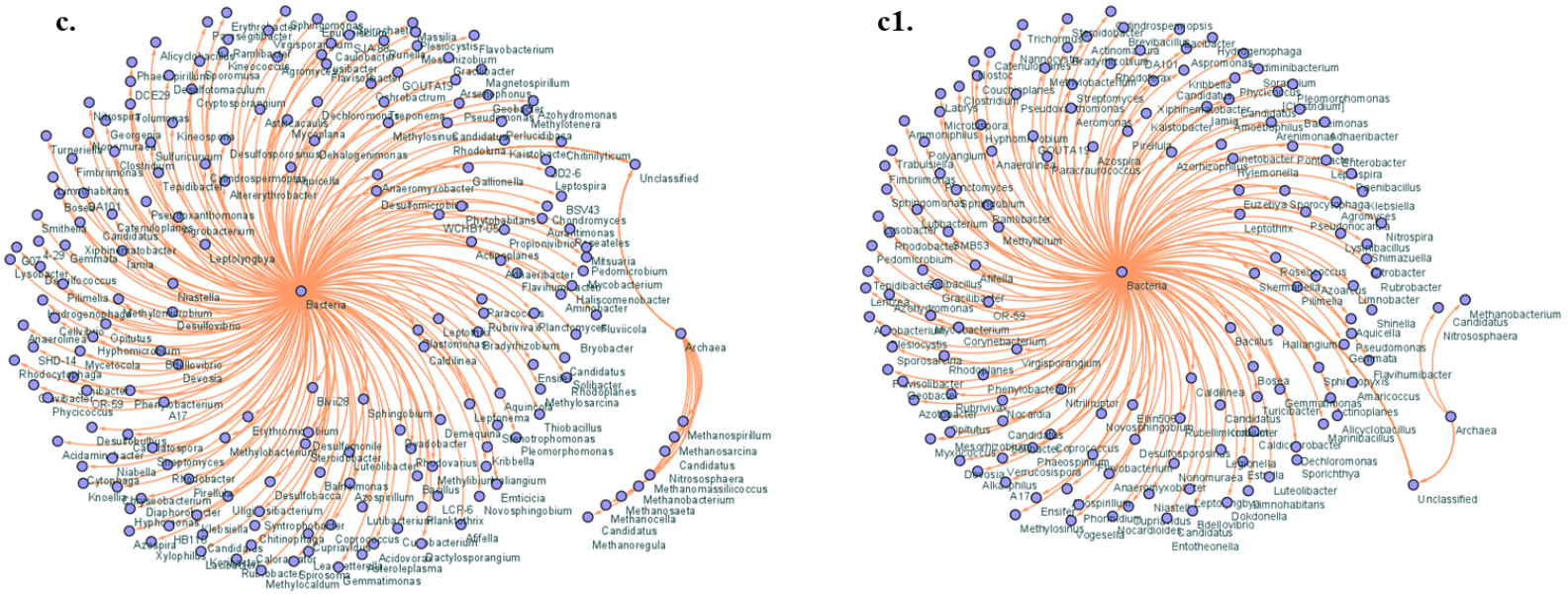

Microbial network analysis of three different phase soils- developing, milking and harvest (**a-a1, b-b1, c-c1**), shows different distribution and connection pattern depending on the selected elemental distribution and content in the field at two different seasonal point of rice cultivation- pre-monsoon (**a, b, c**) and monsoon (**a1, b1, c1**). Nutrient change in the soil system modulates microbial community distribution and this graph shows such interactive patterns. Nodes in these graphs are representing microbial classes and edges are numeric values of element's concentration. These graphs are made using Cytoscape (version 3.8.2).

Effect of combined dry-wet irrigation and microbial dynamics on soil nutrient bioavailability

Contents-

Detailed process of metagenomics study-

- ***DNA extraction from soil and metagenomic library preparation***

A small amount of soil (0.25 gm) was used for the DNA isolation using QiagenDNeasy Powersoil Kit (Cat#12888-50). Soil samples were vortexed for 2 mins within a Powerbead tube in which 60µl of solution C1 was added and vortexed again. Rest of the process was followed according to the kit manufacturer guidelines. 50µl of nuclease free water (Ambion, Cat#AM9938) was used for the DNA elution. Nanodrop 2000 and agarose gel electrophoresis were used for qualitative and quantitative analysis. Region-specific targeting proprietary primers at Genotypic Technology Pvt. Ltd., Bangalore, India, were used for all the metagenomics analysis and V3-V4 metagenome library preparation. All the detailed processes have been mentioned in the supplementary file. Genomic DNA was amplified for 26 cycles (Round 1) using KAPA HiFi HotStart PCR Kit (KAPA Biosystems Inc., Boston, MA USA). Both forward and reverse primer concentrations were 5µM on 1.2% agarose gel bed. PCR amplicons from round 1 (1µl diluted volume) were used for the round 2 PCR indexing, amplified for 10 PCR cycles. Then the loadings were added to the Illumina sequencing barcoded adaptors (Nextera XT v2 Index Kit, Illumina, U.S.A.); another gel electrophoresis was done to normalize and pool the sequenced libraries.

Illumina Adapter Sequences (Majumdar et al., 2020b**):**

5’ -AATGATACGGCGACCACCGAGATCTACAC [i5] TCGTCGGCAGCGTC

5’ -CAAGCAGAAGACGGCATACGAGAT [i7] GTCTCGTGGGCTCGG

[i5, i7] –Unique dual index sequence to identify sample-specific sequencing data.

Samples were then loaded into an Illumina MiSeq v3 600 cycles cartridge (Illumina, CA, USA) and the run was performed according to standard Illumina protocol.

- ***Data output analysis for metagenomics reads***

V3-V4 primer sequence from the Illumina paired-end raw reads were selected from the high quality bases. Further, the reads were joined using Fastq-join. These joined reads were used for the microbiome search using QIIME functions. In further step, query sequences were clustered

using UCLUST process against a trimmed chimera free 16SrRNA database (Greengenes v 13.8). RDP6 classifier was used to assign taxonomies with clustered at ≥97% sequence similarities while comparing to the Greengene database which created a biome file. This biome file was further used for the advanced analysis and visualization. In the biome file, information was stored about the reads number assigned to specific taxa. Microbiome identification and the number of operational taxonomic units (OTUs) for each sample were analyzed using qiime scripts. Calculation of relative abundance from phyla to species from read counts were assigned to OTUs and divided by the total considered reads for the microbiome search. Alpha and beta diversity for microbial species richness were calculated for each sample. Krona charts were made that are interactive html files consisting the phylogenetic information at each taxonomic level. Venn diagram and multivariate analysis were made to identify the difference of microbial diversity in different soil samples.

a.

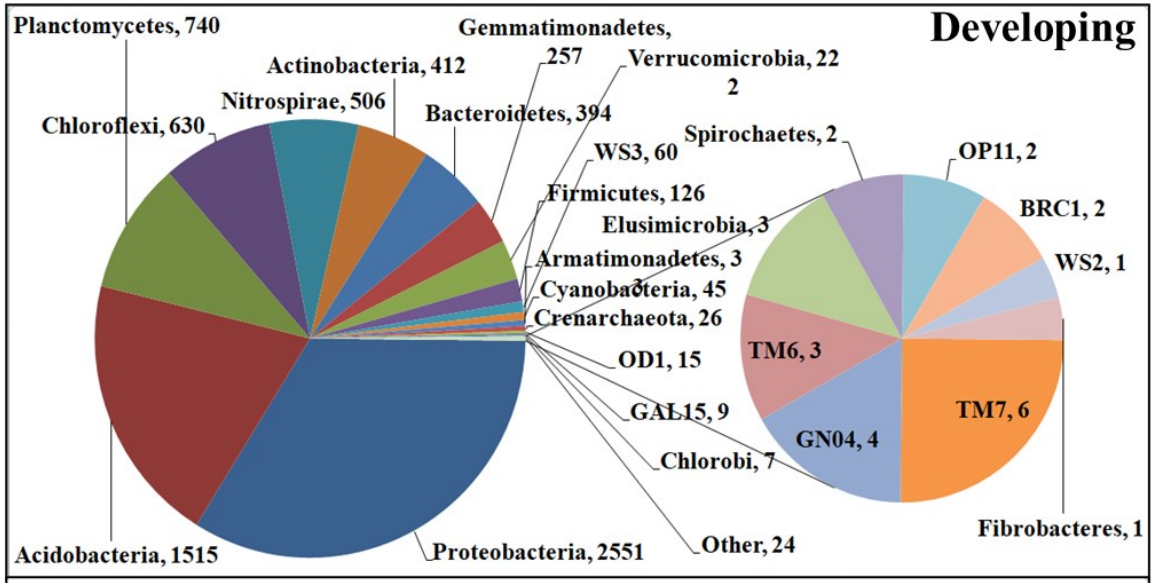
Developing
Planctomycetes, 740
Gemmatimonadetes, 257
Actinobacteria, 412
Verrucomicrobia, 222
Nitrospirae, 506
Bacteroidetes, 394
Chloroflexi, 630
Spirochaetes, 2
OP11, 2
WS3, 60
Firmicutes, 126
BRC1, 2
Elusimicrobia, 3
Armatimonadetes, 33
WS2, 1
Cyanobacteria, 45
Crenarchaeota, 26
TM6, 3
OD1, 15
GAL15, 9
TM7, 6
GN04, 4
Chlorobi, 7
Fibrobacteres, 1
Other, 24
Acidobacteria, 1515
Proteobacteria, 2551

a1.

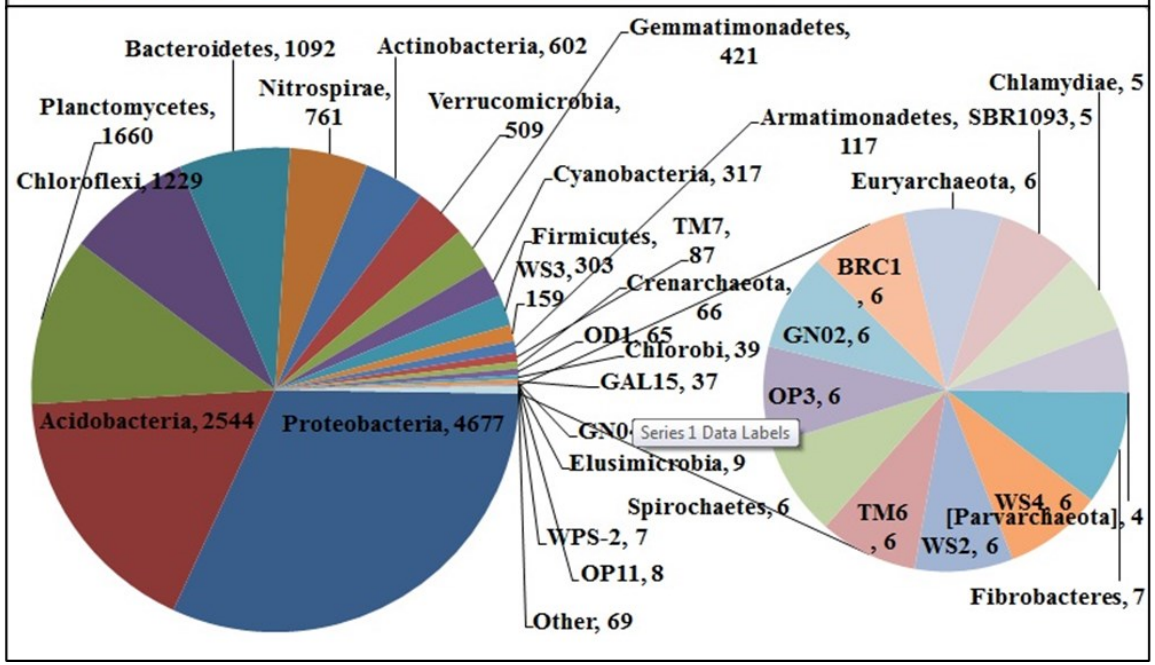
Bacteroidetes, 1092
Actinobacteria, 602
Gemmatimonadetes, 421
Chlamydiae, 5
Nitrospirae, 761
Planctomycetes, 1660
Verrucomicrobia, 509
Armatimonadetes, 117
SBR1093, 5
Cyanobacteria, 317
Euryarchaeota, 6
Chloroflexi, 1229
TM7, 87
Firmicutes, 303
BRC1, 6
WS3, 159
Crenarchaeota, 66
GN02, 6
OD1, 65
Chlorobi, 39
OP3, 6
GAL15, 37
Acidobacteria, 2544
Proteobacteria, 4677
Series 1 Data Labels
Elusimicrobia, 9
Spirochaetes, 6
TM6, 6
WS4, 6
[Parvarchaeota], 4
WS2, 6
WPS-2, 7
OP11, 8
Fibrobacteres, 7
Other, 69

b.

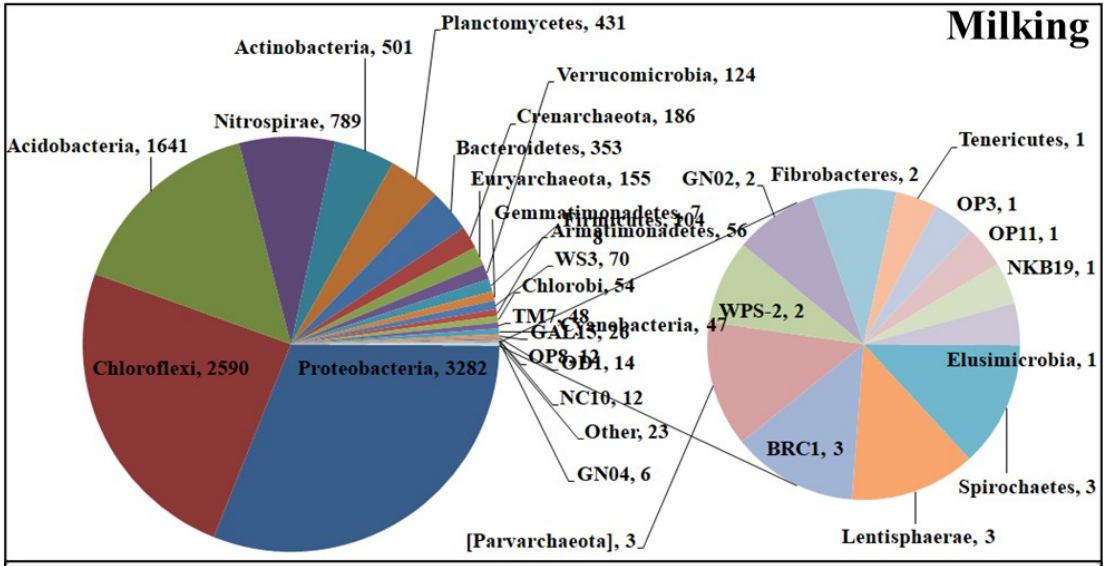
Milking
Planctomycetes, 431
Actinobacteria, 501
Verrucomicrobia, 124
Crenarchaeota, 186
Nitrospirae, 789
Acidobacteria, 1641
Bacteroidetes, 353
Euryarchaeota, 155
GN02, 2
Fibrobacteres, 2
Tenericutes, 1
OP3, 1
OP11, 1
NKB19, 1
WS3, 70
Chlorobi, 54
WPS-2, 2
Elusimicrobia, 1
Chloroflexi, 2590
Proteobacteria, 3282
OD1, 14
NC10, 12
Other, 23
BRC1, 3
GN04, 6
Spirochaetes, 3
[Parvarchaeota], 3
Lentisphaerae, 3

b1.

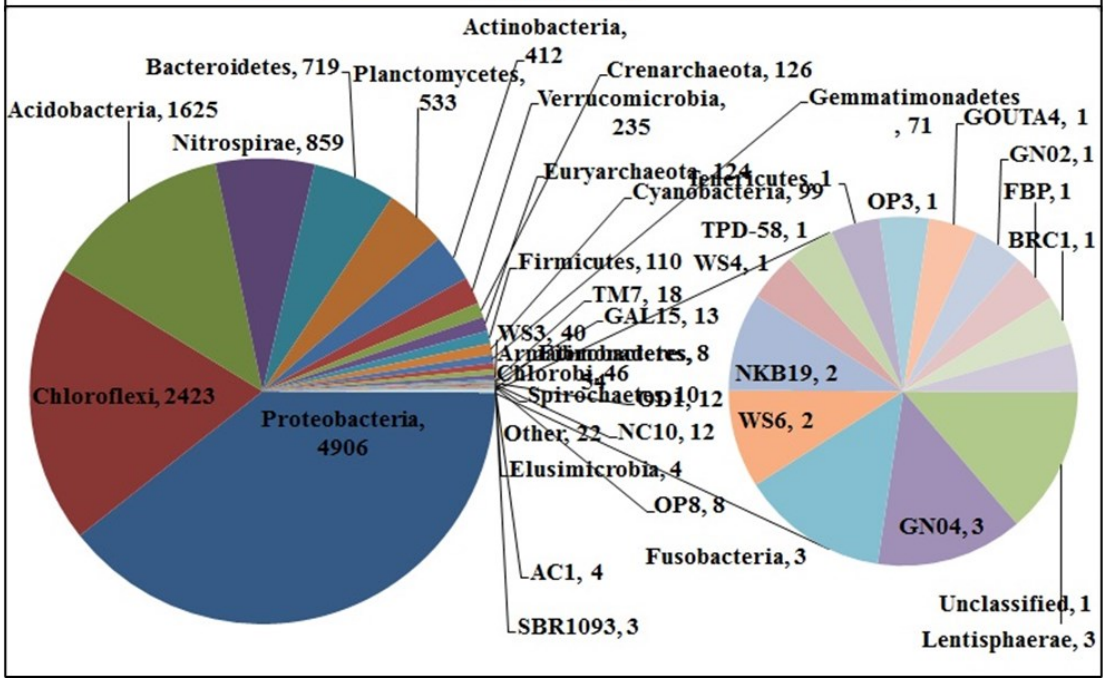
Actinobacteria, 412
Bacteroidetes, 719
Planctomycetes, 533
Crenarchaeota, 126
Verrucomicrobia, 235
Gemmatimonadetes, 71
GOUTA4, 1
Acidobacteria, 1625
Nitrospirae, 859
GN02, 1
Euryarchaeota, 124
Tenericutes, 1
FBP, 1
Cyanobacteria, 99
OP3, 1
TPD-58, 1
BRC1, 1
Firmicutes, 110
WS4, 1
TM7, 18
GAL15, 13
WS3, 40
NKB19, 2
Chlorobi, 46
Chloroflexi, 2423
Spirochaetes, 10
OD1, 12
WS6, 2
Proteobacteria, 4906
Other, 22
NC10, 12
Elusimicrobia, 4
OP8, 8
GN04, 3
Fusobacteria, 3
AC1, 4
Unclassified, 1
SBR1093, 3
Lentisphaerae, 3

c.

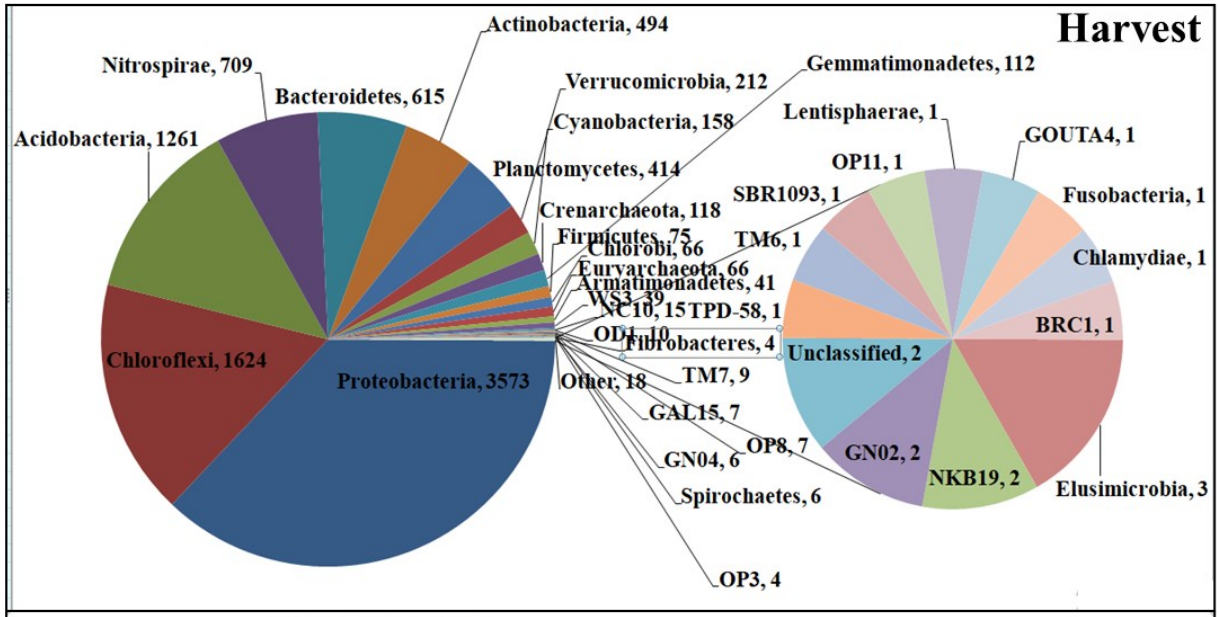
Harvest
Actinobacteria, 494
Nitrospirae, 709
Bacteroidetes, 615
Verrucomicrobia, 212
Gemmatimonadetes, 112
Cyanobacteria, 158
Lentisphaerae, 1
GOUTA4, 1
Acidobacteria, 1261
Planctomycetes, 414
OP11, 1
SBR1093, 1
Fusobacteria, 1
Crenarchaeota, 118
Firmicutes, 75
TM6, 1
Chlamydiae, 1
Chlorobi, 66
Euryarchaeota, 66
Armatimonadetes, 41
WS3, 39
NC10, 15
TPD-58, 1
BRC1, 1
OD1, 10
Fibrobacteres, 4
Unclassified, 2
Chloroflexi, 1624
Proteobacteria, 3573
Other, 18
TM7, 9
GAL15, 7
OP8, 7
GN02, 2
GN04, 6
NKB19, 2
Elusimicrobia, 3
Spirochaetes, 6
OP3, 4

c1.

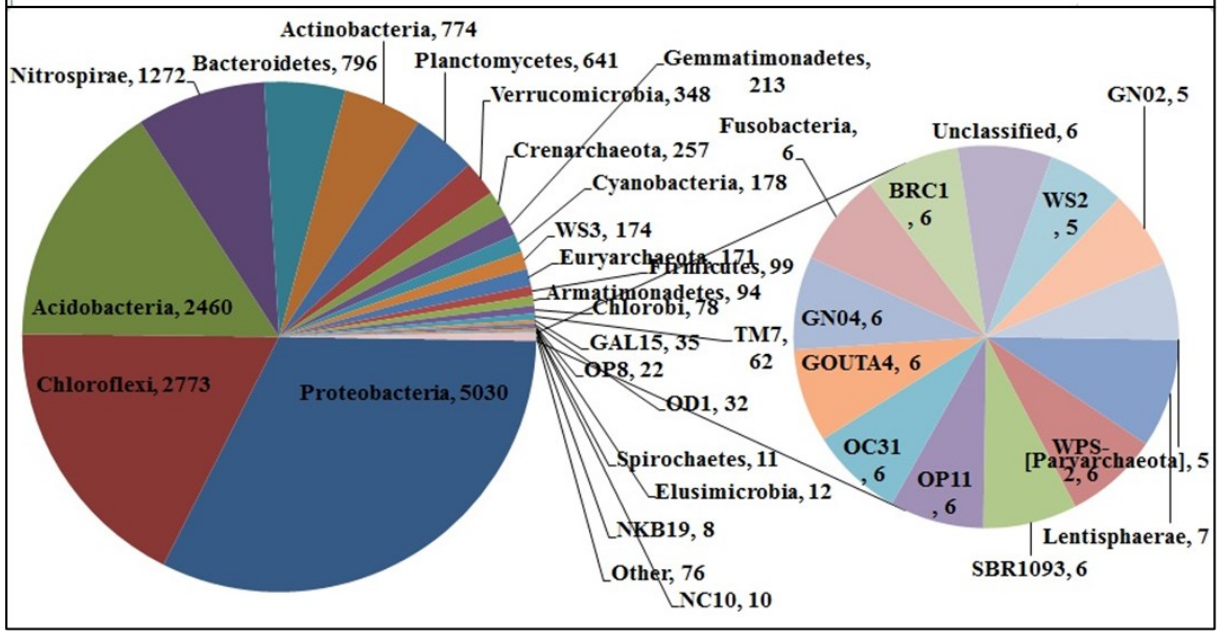
Actinobacteria, 774
Nitrospirae, 1272
Bacteroidetes, 796
Planctomycetes, 641
Gemmatimonadetes, 213
Verrucomicrobia, 348
GN02, 5
Fusobacteria, 6
Unclassified, 6
Crenarchaeota, 257
Cyanobacteria, 178
BRC1, 6
WS2, 5
WS3, 174
Euryarchaeota, 171
Firmicutes, 99
Armatimonadetes, 94
Acidobacteria, 2460
Chlorobi, 78
GN04, 6
TM7, 62
GAL15, 35
GOUTA4, 6
OP8, 22
Chloroflexi, 2773
Proteobacteria, 5030
OD1, 32
OC31, 6
WPS-2, 6
[Parvarchaeota], 5
Spirochaetes, 11
OP11, 6
Elusimicrobia, 12
Lentisphaerae, 7
NKB19, 8
SBR1093, 6
Other, 76
NC10, 10

Supplementary Figure 1. Soil microbial phylum diversity under three field conditions.

Combined soil metagenomics results of soils from three plant growth phases have been represented here in form of special pie chart showing the majority of the microbial phyla encountered with high read numbers in the main pie chart and phyla with low read numbers are casted out as a secondary pie. Observed numbers of read are mentioned alongside of each phylum. Field soils have been cross-checked at two different seasons of pre-monsoon (**a, b, c**) and monsoon (**a1, b1, c1**) to compare any altered microbial community. A higher read was observed during the harvesting phase of rice cultivation.

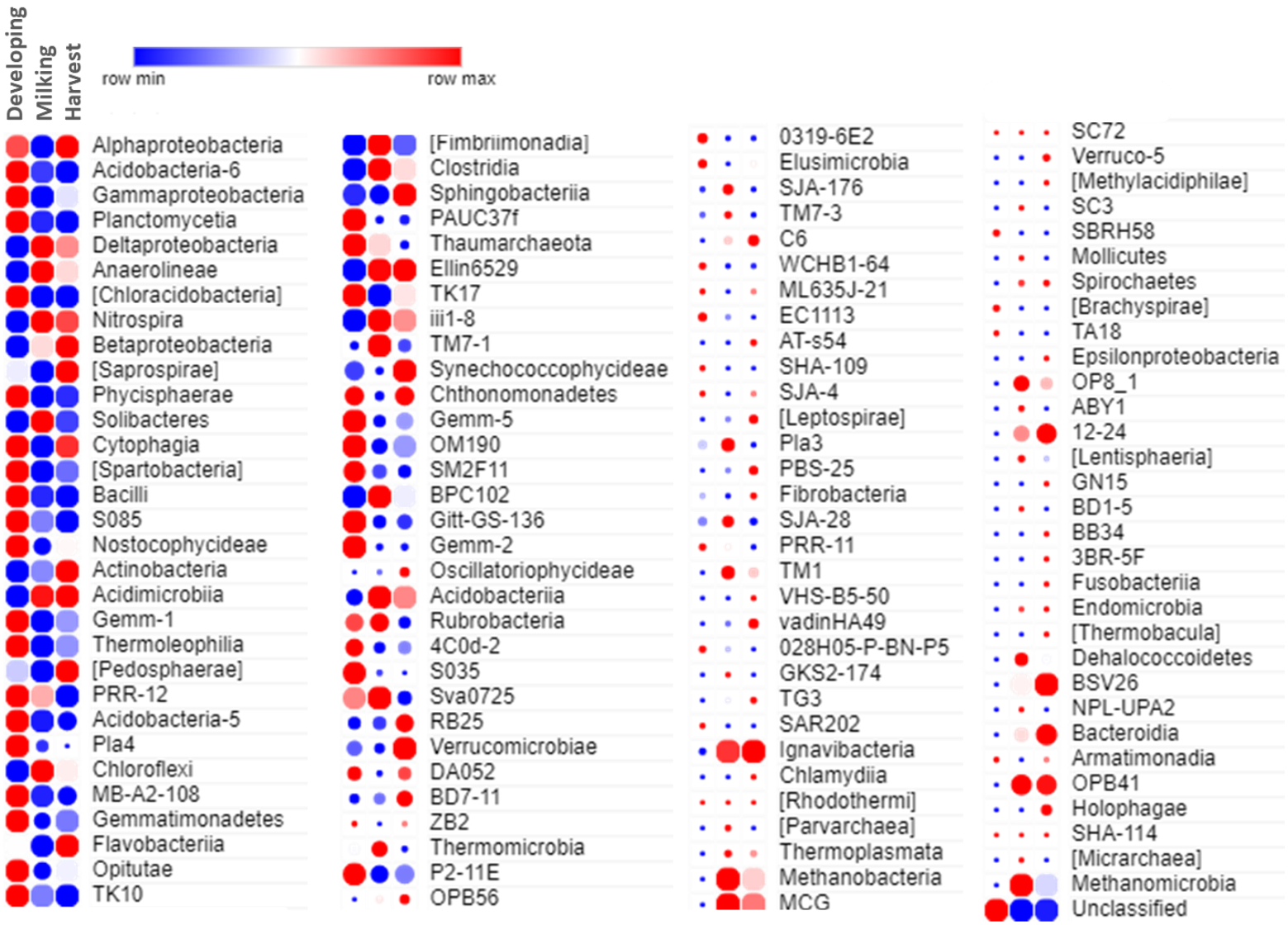

Supplementary Figure 2. Microbial class distribution in three soils with availability and dominance.

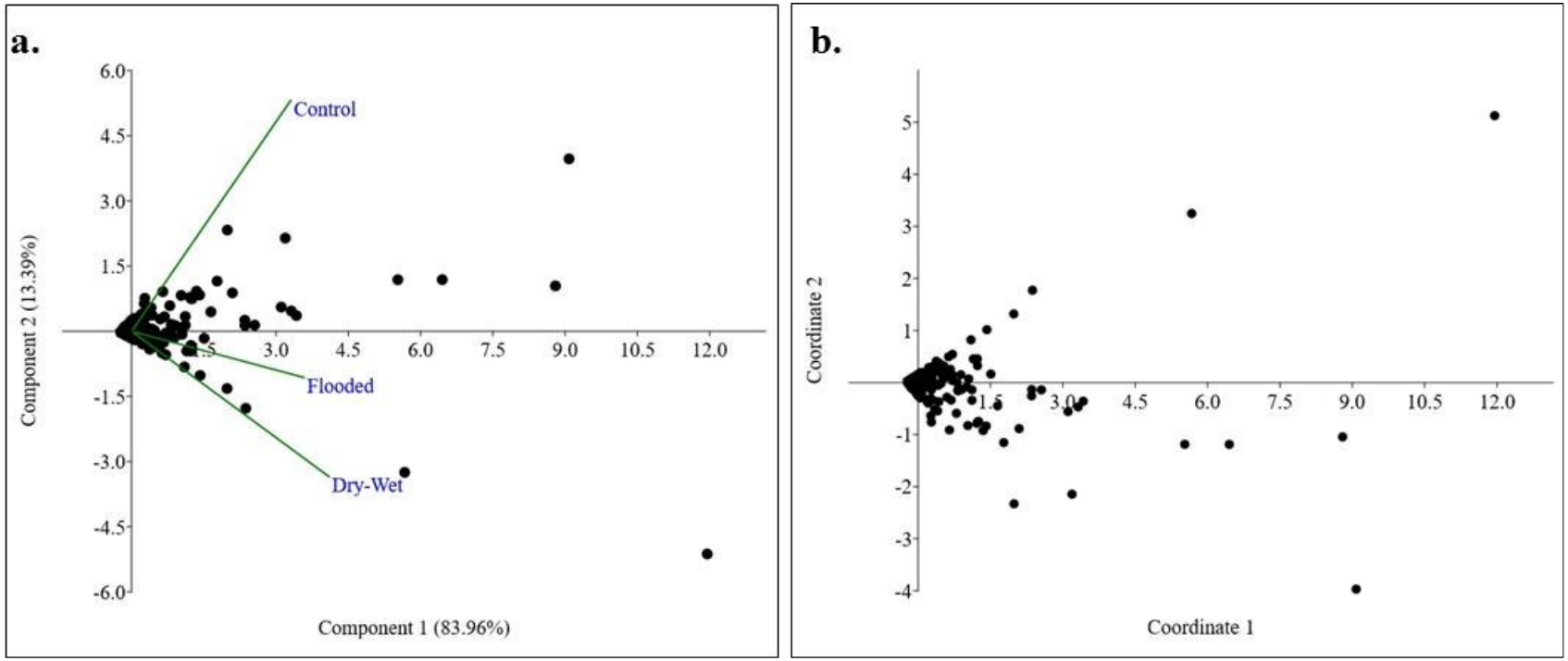

Supplementary Figure 3. Principal component analysis (PCA) (**a**) and principal coordinate analysis (PCoA) (**b**) in three different phase soil microbiomes.

Fraction	Solution	Applied Conditions
F1: Exchangeable	8 ml of $MgCl_2$ (1M, pH=7.0)	1 hr. at Room temperature, continuous agitation
F2: Carbonates	8ml of NaOAc (1M, pH=5.0) w/ CH_3COOH	5 hrs. at Room temperature, continuous agitation
F3: Iron and Manganese Oxides	20ml of NH_2OH*HCl in 25% (v/v) HOAc	6 hrs. at 96°C, intermittent agitation
F4: Organic Matter	3ml of HNO_3 (0.02M)	2 hrs. at 85°C, intermittent agitation
	5ml of 30%H_2O_2 (pH=2) w/HNO_3	
	3ml of 30%H_2O_2 (pH=2) w/HNO_3	3hrs. at 85°C, intermittent agitation
	5ml of NH_4OAc(3.2M) in 20% (v/v)HNO_3 diluted to 20mL with Milli-Q water	30 mins. at Room temperature, continuous agitation
F5: Residual	HF-$HClO_4$ (5 : 1)	-

Supplementary Table 1. Details of sequential extraction analysis method with reactant application dosages.

PARAMETER	ICPMS (Parkin-Elmer)
RF Power	4.2 Kw
Carrier Gas Flow Rate	20 ml/min
Argon Plasma Flow Rate (Nebulizer cold Plasma)	1.01 L/min
Sampling Depth	150 to 180
Collision Cell Gas	He (93%) + H (7%)
Collision Cell Gas Flow Rate	2-10 ml /min
Nebulizer Pump Rate	0.5 rps (30 RPM)
Uptake Time	30 s
Wash Time	60- 70 s

Supplementary Table 2. Instrument specifications during ICP-MS analysis.

Parameters	WD XRF (Bruker S8 Tiger)
Analysis range	Beryllium to Uranium
Sample form	Powder solid
Concentration range	Concentrations from sub ppm to 100%
Sample size	Less than 200mm mess size
Excitation	End window 4kW Rh anode tube (60Kv, 170mA)
Detector gas	P10 gas (10 % methane, 90 % argon)
X-ray Detectors	Gas flow proportional counters and Scintillation counters

Supplementary Table 3. Instrument specifications of Wavelength Dispersive XRF.

Field samples	Alpha diversity indices		
Pre-monsoon	**Shannon**	**Simpson**	**Chao1**
Developing	9.39	0.946	2418.05
Milking	9.18	0.906	2014.34
Harvest	9.69	0.954	2862.10
Monsoon	**Shannon**	**Simpson**	**Chao1**
Developing	8.91	0.822	2314.24
Milking	8.67	0.856	1936.78
Harvest	8.95	0.871	2639.22
	Beta diversity indices		
Pre-monsoon	**Whittaker**	**Cody**	**Williams**
Developing:Milking	0.272	102.5	0.115
Milking:Harvest	0.335	144.5	0.174
Harvest:Developing	0.318	117	0.126
Monsoon	**Shannon**	**Simpson**	**Chao1**
Developing:Milking	0.214	94.25	0.093
Milking:Harvest	0.299	108.61	0.095
Harvest:Developing	0.296	102.97	0.098

Supplementary Table 4. Average Alpha and Beta diversity indices of soil microbiome in three phase samples.